Published by Institute of Physics Publishing for SISSA

Received: *September 12, 2006*
Accepted: *December 23, 2006*
Published: *January 18, 2007*

A subtraction scheme for computing QCD jet cross sections at NNLO: regularization of doubly-real emissions

Gábor Somogyi and Zoltán Trócsányi

University of Debrecen and
Institute of Nuclear Research of the Hungarian Academy of Sciences
H-4001 Debrecen, PO Box 51, Hungary
E-mail: somogyga@dragon.unideb.hu, z.trocsanyi@atomki.hu

Vittorio Del Duca

Istituto Nazionale di Fisica Nucleare, Sez. di Torino
via P. Giuria, 1 – 10125 Torino, Italy
E-mail: delduca@to.infn.it

Abstract: We present a generalization of the dipole subtraction scheme for computing jet cross sections in electron-positron annihilation at next-to-next-to-leading order accuracy in perturbative QCD. In this first part we deal with the regularization of the doubly-real contribution to the NNLO correction.

Keywords: QCD, Jets.

JHEP01(2007)070

Contents

JHEP01(2007)070

1. Introduction

QCD, the theory of strong interactions, is an important component of the Standard Model of elementary particle interactions. It is asymptotically free, which allows us to compute cross sections of elementary particle interactions at high energies as a perturbative expansion in the running strong coupling $\alpha_s(\mu_R)$. However, the running coupling $\alpha_s(\mu_R)$ remains rather large at energies relevant at recent and future colliders. In addition, to leading order in the perturbative expansion, the coupling varies sizeably with the choice of the (unphysical) renormalization scale μ_R. In hadron-initiated processes, the situation is worsened by the dependence of the cross section on the (also unphysical) factorization scale μ_F, which separates the long-distance from the short-distance part of the strong interaction. Thus, a leading-order evaluation of the cross section yields rather unreliable predictions for most processes in the theory. To improve this situation, in the past 25 years the radiative corrections at the next-to-leading order (NLO) accuracy have been computed. These efforts have culminated, when process-independent methods were presented for computing QCD cross sections to NLO accuracy, namely the slicing [1, 2], subtraction [3 – 5] and dipole subtraction [6] methods. In some cases, though, the NLO corrections were found to be disturbingly large, and/or the dependence on μ_R (and eventually μ_F) was found to be still sizeable, thus casting doubts on the applicability of the perturbative predictions. When the NLO corrections are found to be of the same order as the leading-order prediction, the only way to assess the reliability of QCD perturbation theory is the computation of the next-to-next-to-leading order (NNLO) corrections.

In recent years severe efforts have been made to compute the NNLO corrections to the parton distribution functions [7] and important basic processes, such as vector boson production [8 – 12] and Higgs production [9, 13 – 16] in hadron collisions and jet production in electron-positron annihilation [17, 18]. These computations evaluate also the phase space integrals in d dimensions, thus, do not follow the process-independent methods used to compute the NLO corrections.

The more traditional approach relies on defining approximate cross sections which match the singular behaviour of the QCD cross sections in all the relevant unresolved limits. Various attempts were made in this direction in refs. [19 – 29]. In general, the definition of the approximate cross sections must rely on the singly- and doubly-unresolved limits of the QCD squared matrix elements. Although the infrared limits of QCD matrix elements have been extensively studied both at tree-level [30 – 41], and at one-loop [42 – 46], the formulae presented in the literature do not lend themselves directly for devising the approximate cross sections for two reasons. The first problem is that the various single and double soft and/or collinear limits overlap in a very complicated way and the infrared factorization formulae have to be written in such forms that these overlaps can be disentangled so that double subtraction is avoided. The second problem is that even if the factorization formulae are written such that double subtraction does not happen, the expressions cannot straightforwardly be used as subtraction formulae, because the momenta of the partons in the factorized matrix elements are unambiguously defined only in the strict soft and collinear limits. In order to define the approximate cross sections one also has to factorize

JHEP01(2007)070

the phase space of the unresolved partons such that the singular factors can be integrated and the remaining expressions can be combined with the virtual correction leading to cross sections which are finite and integrable in four dimensions.

In ref. [47] we presented a solution to the first problem, but did not explicitly define the approximate cross sections, which we left for later work. In this paper we turn to the second problem and define the complete approximate cross sections that regularize the doubly-real emission. For factorizing the phase space one has two options. On the one hand we may decompose the squared matrix elements into expressions that contain only single singular factors and use the factorization formulae as subtraction terms. In NLO computations this method was termed 'residuum subtraction'. On the other hand one may use exact phase-space factorization (keeping momentum conservation and particles on-shell) to maintain gauge invariance of the factorized matrix elements. In NLO computations the 'dipole subtraction method' represents an example of this approach.

The single singular factor decomposition cannot be followed in a NNLO computation because a singular factor in a doubly-unresolved region of the phase space naturally contains singular factors in singly-unresolved regions. Therefore, we have to use exact factorizations of the unresolved phase space measures. There are only two known ways of exact phase space factorization, one termed 'dipole factorization' [6], while the other called 'antennae factorization' [19]. Actually, both belong to the same general class. The important feature of these is that in order to factorize the unresolved phase space measures, two partons, called 'emitter' and 'spectator', are singled out for each subtraction term. The emitter emits the unresolved parton and the spectator takes away the momentum recoil to maintain momentum conservation. In a NLO computation the choice for the emitter-spectator pair is naturally a colour-connected pair of partons in the soft factorization formula. The collinear emissions are distributed among the soft ones using colour conservation. Although this trick provides a fairly elegant framework for computing NLO corrections, the unnatural distribution of collinear emissions seems impossible to maintain in a NNLO computation because it leads to simultaneously spin- and colour-correlated squared matrix elements for which collinear factorization formulae do not exist [47].[1]

In ref. [28] the antennae factorization is used for NNLO subtractions, which is made possible by the use of colour-ordered subamplitudes, where the emitter-spectator 'antenna pairs' can naturally and unambiguously be selected because singular emission for a given amplitude can occur only between ordered pairs of momenta (the emitter and the spectator). Note however, that the effect of quantum interference in the squared matrix element mixes the colour subamplitudes in a rather complicated way and a general scheme to construct the subtraction terms in a process-independent way has not been given yet. It seems to us that in order to construct a general method for computing NNLO corrections we are forced to generalize the dipole factorizations of the phase space such that for each subtraction term all partons of the whole event, except the emitter and the unresolved ones, play the role of spectators democratically.

In ref. [48], we defined a new NLO subtraction scheme with exact phase-space factoriza-

[1]Note a misprint in ref. [47], where 'soft' factorization is written in this respect instead of 'collinear'.

JHEP01(2007)070

tion based on the generalized dipole factorization mentioned above. Formally, that scheme can easily be generalized to any order in perturbation theory. In this paper we extend that scheme to computing the contribution of the doubly-real emission to the NNLO corrections. We demonstrate that the regularized cross section is indeed numerically integrable by computing the corresponding contribution to the cross section of electron-positron annihilation into three jets from the $e^+e^- \to q\bar{q}ggg$ subprocess.

2. Jet cross sections at NNLO accuracy

The jet cross sections in perturbative QCD are represented by an expansion in the strong coupling α_s. At NNLO accuracy we keep the three lowest-order terms,

$$\sigma = \sigma^{\mathrm{LO}} + \sigma^{\mathrm{NLO}} + \sigma^{\mathrm{NNLO}} . \tag{2.1}$$

Assuming an m-jet quantity, the leading-order contribution is the integral of the fully differential Born cross section $\mathrm{d}\sigma_m^{\mathrm{B}}$ of m final-state partons over the available m-parton phase space defined by the jet function J_m,

$$\sigma^{\mathrm{LO}} = \int_m \mathrm{d}\sigma_m^{\mathrm{B}} J_m . \tag{2.2}$$

The NLO contribution is a sum of two terms, the real and virtual corrections,

$$\sigma^{\mathrm{NLO}} = \int_{m+1} \mathrm{d}\sigma_{m+1}^{\mathrm{R}} J_{m+1} + \int_m \mathrm{d}\sigma_m^{\mathrm{V}} J_m . \tag{2.3}$$

Here the notation for the integrals indicates that the real correction involves $m+1$ final-state partons, one of those being unresolved, while the virtual correction has m-parton kinematics. The NNLO correction is a sum of three contributions, the doubly-real, the one-loop singly-unresolved real-virtual and the two-loop doubly-virtual terms,

$$\sigma^{\mathrm{NNLO}} = \int_{m+2} \mathrm{d}\sigma_{m+2}^{\mathrm{RR}} J_{m+2} + \int_{m+1} \mathrm{d}\sigma_{m+1}^{\mathrm{RV}} J_{m+1} + \int_m \mathrm{d}\sigma_m^{\mathrm{VV}} J_m . \tag{2.4}$$

Here the notation for the integrals indicates that the doubly-real corrections involve $m+2$ final-state partons, the real-virtual contribution involves $m+1$ final-state partons and the doubly-virtual term is an integral over the phase space of m partons, and the phase spaces are restricted by the corresponding jet functions J_n that define the physical quantity.

In $d = 4$ dimensions the two contributions in eq. (2.3) as well as the three contributions in eq. (2.4) are separately divergent, but their sum is finite for infrared-safe observables order by order in the expansion in α_s. The requirement of infrared-safety puts constraints on the analytic behaviour of the jet functions that were spelled out explicitly in ref. [47].

Following from kinematical reasons, fully inclusive observables can be accurately evaluated in QCD perturbation theory relatively simply. Since these observables are completely inclusive, no phase-space restriction has to be applied ($J_n = 1$ for any n). Real and virtual contributions can be combined at the integrand level resulting in the cancellation of soft and collinear singularities before performing the relevant phase-space integrations. Owing

to these features, general techniques have been available for some time [51, 52] to carry out NNLO calculations in analytic form.

QCD calculations beyond LO for inclusive quantities, such as jet cross sections or event-shape distributions, are much more involved. Owing to the complicated phase space for multiparton configurations, analytic calculations are impossible for most of the distributions. Moreover, soft and collinear singularities are separately present in the real radiation correction (due to integrations over the phase space of the unresolved parton) and virtual contributions (due to integrations over the loop momentum) at the intermediate steps. These singularities have to be first regularized by analytic continuation in a number of space-time dimensions $d = 4 - 2\varepsilon$ different from four. This analytic continuation prevents a straightforward implementation of numerical integration techniques.

The traditional approach to finding the finite corrections at NLO accuracy is to regularize the real radiation contribution by subtracting a suitably defined approximate cross section $\mathrm{d}\sigma^{\mathrm{R,A}}$ such that (i) $\mathrm{d}\sigma^{\mathrm{R,A}}$ matches the pointwise singular behaviour of $\mathrm{d}\sigma^{\mathrm{R}}$ in the one-parton infrared regions of the phase space in any dimensions (ii) and it can be integrated over the one-parton phase space of the unresolved parton independently of the jet function, resulting in a Laurent expansion in ε. After performing this integration, the approximate cross section can be combined with the virtual correction $\mathrm{d}\sigma^{\mathrm{V}}$ before integration. We then write

$$\sigma^{\mathrm{NLO}} = \int_{m+1} \left[\mathrm{d}\sigma^{\mathrm{R}}_{m+1} J_{m+1} - \mathrm{d}\sigma^{\mathrm{R,A}}_{m+1} J_m \right] + \int_m \left[\mathrm{d}\sigma^{\mathrm{V}}_m + \int_1 \mathrm{d}\sigma^{\mathrm{R,A}}_{m+1} \right] J_m \,, \tag{2.5}$$

where both integrals on the right-hand side are finite in $d = 4$ dimensions. The form of the subtraction term in eq. (2.5) is symbolic in the sense that it is actually a sum of different terms. The jet function depends on different momenta in each of these terms, the exact set of momenta for each term can be found in ref. [48]. The final result is that one is able to rewrite the two NLO contributions in eq. (2.3) as a sum of two finite integrals,

$$\sigma^{\mathrm{NLO}} = \int_{m+1} \mathrm{d}\sigma^{\mathrm{NLO}}_{m+1} + \int_m \mathrm{d}\sigma^{\mathrm{NLO}}_m \,, \tag{2.6}$$

that are integrable in four dimensions using standard numerical techniques.

The construction of the suitable approximate cross section $\mathrm{d}\sigma^{\mathrm{R,A}}$ is made possible by the universal soft and collinear factorization properties of QCD matrix elements. Envisaging a similar construction for computing the NNLO correction, the universal infrared behaviour of the loop amplitudes and the infrared limits of the real-emission corrections at NNLO, as well as the singularity structure of the two-loop squared matrix elements has been computed [49, 50]. However, it is far more complex to disentangle these singularities at the NNLO accuracy than at NLO [47], thus up to now, process independent approximate cross sections for regularizing the $\mathrm{d}\sigma^{\mathrm{RR}}$ and $\mathrm{d}\sigma^{\mathrm{RV}}$ terms have not been computed, but for the relatively simple case of $e^+e^- \to 2$ and 3 jets, when the dependence on colour completely factorizes from all matrix elements [24, 29].

In order to avoid this complexity in ref. [53] a new method has been developed for computing the QCD corrections by combining the real-emission and virtual corrections

before integration for arbitrary jet function. The method is very simple conceptually. It considers the problem from a purely mathematical point of view: how to compute a complicated, but finite integral numerically? The first step is to map the phase spaces onto the unit hypercube of suitable dimensions. Then the singularities from inside the hypercube are removed to the edges of the cube by splitting appropriately the integrations and mapping them back to the $[0,1]$ interval. Next, the overlapping singularities are disentangled using sector decomposition [54 – 59]. At this point the only factors in the integrand that lead to divergences are of the form $\lambda^{-1+n\varepsilon}$, therefore, the ε poles can be extracted in terms of plus distributions [53]. The method is clearly completely general and its strength has already been demonstrated in various explicit computations [15 – 17, 12]. Note however, that the various mappings of the phase space as well as the sector decompositions are not unique. The particular choices depend on the analytic structure of the functions one has to integrate, namely, the squared matrix elements for the given process. In fact, the different terms in the squared matrix element may prefer different mappings as in the case of ref. [16]. This means that with this technique the construction of a universal program that requires only various matrix elements as input for computing NNLO corrections for arbitrary processes does not seem straightforward.

Such program exists for computing NLO corrections [60 – 62] based upon the subtraction method. Therefore, it is of interest whether the subtraction method can be extended to the computation of NNLO corrections. In the next section we rewrite eq. (2.4) such that each phase space integral is finite and thus can be performed numerically in four dimensions using standard Monte Carlo techniques.

3. Subtraction scheme at NNLO accuracy

Let us consider first the doubly-real contribution, $\mathrm{d}\sigma^{\mathrm{RR}}_{m+2}$. It is divergent in the doubly-unresolved regions of phase space. In order to cancel the two-parton singularities we subtract the approximate cross section $\mathrm{d}\sigma^{\mathrm{RR,A_2}}_{m+2}$ that matches the pointwise singular behaviour of $\mathrm{d}\sigma^{\mathrm{RR}}_{m+2}$ in d dimensions in the two-parton infrared regions. Then we have

$$\begin{aligned}\sigma^{\mathrm{NNLO}} = &\int_{m+2}\Big[\mathrm{d}\sigma^{\mathrm{RR}}_{m+2}J_{m+2} - \mathrm{d}\sigma^{\mathrm{RR,A_2}}_{m+2}J_m\Big] \\ &+ \int_{m+1}\mathrm{d}\sigma^{\mathrm{RV}}_{m+1}J_{m+1} + \int_m\Big[\mathrm{d}\sigma^{\mathrm{VV}}_m + \int_2\mathrm{d}\sigma^{\mathrm{RR,A_2}}_{m+2}\Big]J_m\,. \end{aligned} \tag{3.1}$$

However the first integral is still divergent in the singly-unresolved regions of the phase space. In order to cancel these remaining singularities we subtract the approximate cross sections $\mathrm{d}\sigma^{\mathrm{RR,A_1}}_{m+2}$ and $\mathrm{d}\sigma^{\mathrm{RR,A_{12}}}_{m+2}$ to obtain

$$\begin{aligned}\sigma^{\mathrm{NNLO}} = &\int_{m+2}\Big[\mathrm{d}\sigma^{\mathrm{RR}}_{m+2}J_{m+2} - \mathrm{d}\sigma^{\mathrm{RR,A_2}}_{m+2}J_m - \Big(\mathrm{d}\sigma^{\mathrm{RR,A_1}}_{m+2}J_{m+1} - \mathrm{d}\sigma^{\mathrm{RR,A_{12}}}_{m+2}J_m\Big)\Big] \\ &+ \int_{m+1}\Big[\mathrm{d}\sigma^{\mathrm{RV}}_{m+1} + \int_1\mathrm{d}\sigma^{\mathrm{RR,A_1}}_{m+2}\Big]J_{m+1} \\ &+ \int_m\Big[\mathrm{d}\sigma^{\mathrm{VV}}_m + \int_2\mathrm{d}\sigma^{\mathrm{RR,A_2}}_{m+2} - \int_2\mathrm{d}\sigma^{\mathrm{RR,A_{12}}}_{m+2}\Big]J_m\,. \end{aligned} \tag{3.2}$$

Here $\mathrm{d}\sigma^{\mathrm{RR},\mathrm{A}_1}_{m+2}$ and $\mathrm{d}\sigma^{\mathrm{RR},\mathrm{A}_{12}}_{m+2}$ regularize the singly-unresolved limits of $\mathrm{d}\sigma^{\mathrm{RR}}_{m+2}$ and $\mathrm{d}\sigma^{\mathrm{RR},\mathrm{A}_2}_{m+2}$ respectively. For the construction to be consistent, we must also require that $\mathrm{d}\sigma^{\mathrm{RR},\mathrm{A}_1}_{m+2} - \mathrm{d}\sigma^{\mathrm{RR},\mathrm{A}_{12}}_{m+2}$ be integrable in the two-parton infrared regions of the phase space,[2] which restricts the possible forms of $\mathrm{d}\sigma^{\mathrm{RR},\mathrm{A}_{12}}_{m+2}$ severely. In eq. (3.2) the jet functions, multiplying each approximate cross section, organize the terms according to in which integral they should appear. In particular, $\mathrm{d}\sigma^{\mathrm{RR},\mathrm{A}_1}_{m+2}$ is multiplied by J_{m+1}, therefore, after integration over the phase space of the unresolved parton, it is combined with $\mathrm{d}\sigma^{\mathrm{RV}}_{m+1}$, while $\mathrm{d}\sigma^{\mathrm{RR},\mathrm{A}_{12}}_{m+2}$ is multiplied with J_m, therefore, it is added back in the third line. The $m+2$-parton integral above is now finite by construction.

Next consider the real-virtual contribution $\mathrm{d}\sigma^{\mathrm{RV}}_{m+1}$. It has two types of singularities: (i) explicit ε poles in the loop amplitude and (ii) kinematical singularities in the singly-unresolved regions of the phase space. In eq. (3.2) the former are already regularized. Indeed, unitarity guarantees that the second line of that equation is free of ε poles if $\mathrm{d}\sigma^{\mathrm{RR},\mathrm{A}_1}_{m+2}$ is a true regulator of $\mathrm{d}\sigma^{\mathrm{RR}}_{m+2}$ in the one-parton infrared regions of the phase space, just as it does in NLO subtraction schemes. To regularize the kinematical singularities, we subtract the approximate cross sections $\mathrm{d}\sigma^{\mathrm{RV},\mathrm{A}_1}_{m+1}$ and $\left(\int_1 \mathrm{d}\sigma^{\mathrm{RR},\mathrm{A}_1}_{m+2}\right)^{\mathrm{A}_1}$, which regularize the real-virtual cross section $\mathrm{d}\sigma^{\mathrm{RV}}_{m+1}$ and $\int_1 \mathrm{d}\sigma^{\mathrm{RR},\mathrm{A}_1}_{m+2}$, respectively, when a single parton becomes unresolved. Thus, the NNLO cross section is written as

$$\begin{aligned}\sigma^{\mathrm{NNLO}} = &\int_{m+2}\Big\{\mathrm{d}\sigma^{\mathrm{RR}}_{m+2}J_{m+2} - \mathrm{d}\sigma^{\mathrm{RR},\mathrm{A}_2}_{m+2}J_m - \Big[\mathrm{d}\sigma^{\mathrm{RR},\mathrm{A}_1}_{m+2}J_{m+1} - \mathrm{d}\sigma^{\mathrm{RR},\mathrm{A}_{12}}_{m+2}J_m\Big]\Big\}_{\varepsilon=0} \\ &+\int_{m+1}\Big\{\Big(\mathrm{d}\sigma^{\mathrm{RV}}_{m+1}+\int_1 \mathrm{d}\sigma^{\mathrm{RR},\mathrm{A}_1}_{m+2}\Big)J_{m+1} - \Big[\mathrm{d}\sigma^{\mathrm{RV},\mathrm{A}_1}_{m+1}+\Big(\int_1 \mathrm{d}\sigma^{\mathrm{RR},\mathrm{A}_1}_{m+2}\Big)^{\mathrm{A}_1}\Big]J_m\Big\}_{\varepsilon=0} \\ &+\int_m\Big\{\mathrm{d}\sigma^{\mathrm{VV}}_m + \int_2\Big[\mathrm{d}\sigma^{\mathrm{RR},\mathrm{A}_2}_{m+2} - \mathrm{d}\sigma^{\mathrm{RR},\mathrm{A}_{12}}_{m+2}\Big] + \int_1\Big[\mathrm{d}\sigma^{\mathrm{RV},\mathrm{A}_1}_{m+1}+\Big(\int_1 \mathrm{d}\sigma^{\mathrm{RR},\mathrm{A}_1}_{m+2}\Big)^{\mathrm{A}_1}\Big]\Big\}_{\varepsilon=0}J_m\,.\end{aligned} \tag{3.3}$$

Since the first and second integrals on the right hand side of this equation are finite in $d=4$ dimensions by construction, it follows from the Kinoshita-Lee-Nauenberg theorem that the combination of integrals in the last line is finite as well, provided the jet function defines an infrared-safe observable. We should like to emphasize that the form of the subtraction terms in the first two lines of eq. (3.3) is symbolic in the sense that a single subtraction term is actually a sum of different terms. The jet function depends on different momenta in each of these terms. The exact set of momenta for each term in the first line will be presented in sections 5–7 and for the second line in a separate publication.

The final result of these manipulations is that we rewrite eq. (2.4) as

$$\sigma^{\mathrm{NNLO}} = \int_{m+2}\mathrm{d}\sigma^{\mathrm{NNLO}}_{m+2} + \int_{m+1}\mathrm{d}\sigma^{\mathrm{NNLO}}_{m+1} + \int_m \mathrm{d}\sigma^{\mathrm{NNLO}}_m\,, \tag{3.4}$$

that is a sum of three integrals,

$$\mathrm{d}\sigma^{\mathrm{NNLO}}_{m+2} = \Big\{\mathrm{d}\sigma^{\mathrm{RR}}_{m+2}J_{m+2} - \mathrm{d}\sigma^{\mathrm{RR},\mathrm{A}_2}_{m+2}J_m - \Big[\mathrm{d}\sigma^{\mathrm{RR},\mathrm{A}_1}_{m+2}J_{m+1} - \mathrm{d}\sigma^{\mathrm{RR},\mathrm{A}_{12}}_{m+2}J_m\Big]\Big\}_{\varepsilon=0}\,, \tag{3.5}$$

$$\mathrm{d}\sigma^{\mathrm{NNLO}}_{m+1} = \Big\{\Big[\mathrm{d}\sigma^{\mathrm{RV}}_{m+1}+\int_1 \mathrm{d}\sigma^{\mathrm{RR},\mathrm{A}_1}_{m+2}\Big]J_{m+1} - \Big[\mathrm{d}\sigma^{\mathrm{RV},\mathrm{A}_1}_{m+1}+\Big(\int_1 \mathrm{d}\sigma^{\mathrm{RR},\mathrm{A}_1}_{m+2}\Big)^{\mathrm{A}_1}\Big]J_m\Big\}_{\varepsilon=0}\,, \tag{3.6}$$

[2]Formally this means that $\mathrm{d}\sigma^{\mathrm{RR},\mathrm{A}_{12}}_{m+2} = \mathrm{d}\sigma^{\mathrm{RR},\mathrm{A}_{21}}_{m+2}$, which we have already taken into account in writing the expressions.

JHEP01(2007)070

and

$$\mathrm{d}\sigma_m^{\mathrm{NNLO}} = \Big\{\mathrm{d}\sigma_m^{\mathrm{VV}} + \int_2 \Big[\mathrm{d}\sigma_{m+2}^{\mathrm{RR,A_2}} - \mathrm{d}\sigma_{m+2}^{\mathrm{RR,A_{12}}}\Big] + \int_1 \Big[\mathrm{d}\sigma_{m+1}^{\mathrm{RV,A_1}} + \Big(\int_1 \mathrm{d}\sigma_{m+2}^{\mathrm{RR,A_1}}\Big)^{\mathrm{A_1}}\Big]\Big\}_{\varepsilon=0} J_m\,, \tag{3.7}$$

each integrable in four dimensions using standard numerical techniques.

The subtraction scheme presented here differs somewhat from the one outlined in ref. [47], where we assumed that $\mathrm{d}\sigma_{m+2}^{\mathrm{RR,A_{12}}}$ can be defined such that (in the present notation)

$$\int_{m+1} \left[\int_1 \mathrm{d}\sigma_{m+2}^{\mathrm{RR,A_{12}}} - \Big(\int_1 \mathrm{d}\sigma_{m+2}^{\mathrm{RR,A_1}}\Big)^{\mathrm{A_1}}\right] J_m = \text{finite} \tag{3.8}$$

in $d = 4$ dimensions. However, as already emphasized in ref. [47], eq. (3.8) does not follow from unitarity, rather it is a constraint on the definitions of $\mathrm{d}\sigma_{m+2}^{\mathrm{RR,A_1}}$ and $\mathrm{d}\sigma_{m+2}^{\mathrm{RR,A_{12}}}$. It turns out more convenient to drop this extra condition and rearrange the subtraction scheme as presented here.

In this paper we present all formulae relevant for constructing $\mathrm{d}\sigma_{m+2}^{\mathrm{NNLO}}$ explicitly. The terms needed for defining $\mathrm{d}\sigma_{m+1}^{\mathrm{NNLO}}$ and $\mathrm{d}\sigma_m^{\mathrm{NNLO}}$ will be given in separate papers. We use the colour- and spin-state notation introduced in ref. [6]. The complete description of our notation can be found in ref. [47].

4. Subtraction terms for doubly-real emission

The cross section $\mathrm{d}\sigma_{m+2}^{\mathrm{RR}}$ is the integral of the tree-level squared matrix element for $m+2$ parton production over the $m+2$ parton phase space

$$\mathrm{d}\sigma_{m+2}^{\mathrm{RR}} = \mathrm{d}\phi_{m+2} |\mathcal{M}_{m+2}^{(0)}|^2\,, \tag{4.1}$$

where the phase-space measure is defined as

$$\mathrm{d}\phi_n(p_1,\ldots,p_n;Q) = \prod_{i=1}^{n} \frac{\mathrm{d}^d p_i}{(2\pi)^{d-1}} \delta_+(p_i^2)\,(2\pi)^d\,\delta^{(d)}\left(Q - \sum_{i=1}^{n} p_i\right). \tag{4.2}$$

In eq. (4.1) (and all subsequent formulae) the superscript (0) refers to tree-level expressions. We disentangled the overlap structure of the singularities of $|\mathcal{M}_{m+2}^{(0)}|^2$ into the pieces $\mathbf{A}_2|\mathcal{M}_{m+2}^{(0)}|^2$, $\mathbf{A}_1|\mathcal{M}_{m+2}^{(0)}|^2$ and $\mathbf{A}_{12}|\mathcal{M}_{m+2}^{(0)}|^2$ in ref. [47]. These expressions are only defined in the strict soft and/or collinear limits. To define true counterterms, they need to be extended over the full phase space. This extension requires a phase-space factorization that maintains momentum conservation exactly, but such that in addition it respects the delicate structure of cancellations among the various subtraction terms.

The true (extended) counterterms may symbolically be written as

$$\mathrm{d}\sigma_{m+2}^{\mathrm{RR,A_2}} = \mathrm{d}\phi_m\,[\mathrm{d}p_2]\,\boldsymbol{\mathcal{A}}_2 |\mathcal{M}_{m+2}^{(0)}|^2\,, \tag{4.3}$$

$$\mathrm{d}\sigma_{m+2}^{\mathrm{RR,A_1}} = \mathrm{d}\phi_{m+1}\,[\mathrm{d}p_1]\,\boldsymbol{\mathcal{A}}_1 |\mathcal{M}_{m+2}^{(0)}|^2\,, \tag{4.4}$$

and

$$\mathrm{d}\sigma_{m+2}^{\mathrm{RR,A_{12}}} = \mathrm{d}\phi_m\,[\mathrm{d}p_1]\,[\mathrm{d}p_1]\,\boldsymbol{\mathcal{A}}_{12} |\mathcal{M}_{m+2}^{(0)}|^2\,, \tag{4.5}$$

where in eqs. (4.3)–(4.5) we used a formal, calligraphic notation (to be defined explicitly below) to indicate the extension of the terms $\mathbf{A}_2|\mathcal{M}^{(0)}_{m+2}|^2$, $\mathbf{A}_1|\mathcal{M}^{(0)}_{m+2}|^2$ and $\mathbf{A}_{12}|\mathcal{M}^{(0)}_{m+2}|^2$ over the whole phase space that was written in exactly factorized forms,

$$\mathrm{d}\phi_{m+2} = \mathrm{d}\phi_m\,[\mathrm{d}p_2] = \mathrm{d}\phi_{m+1}\,[\mathrm{d}p_1] = \mathrm{d}\phi_m\,[\mathrm{d}p_1]\,[\mathrm{d}p_1] \tag{4.6}$$

(the precise meaning of the factors $[\mathrm{d}p_1]$ and $[\mathrm{d}p_2]$ will be given below).

5. Singly-unresolved counterterms

The singly-unresolved counterterm $\boldsymbol{\mathcal{A}}_1|\mathcal{M}^{(0)}_{m+2}|^2$ reads

$$\boldsymbol{\mathcal{A}}_1|\mathcal{M}^{(0)}_{m+2}(\{p\})|^2 = \sum_r \left[\sum_{i\neq r}\frac{1}{2}\mathcal{C}^{(0,0)}_{ir}(\{p\}) + \left(\mathcal{S}^{(0,0)}_r(\{p\}) - \sum_{i\neq r}\mathcal{C}_{ir}\mathcal{S}^{(0,0)}_r(\{p\})\right)\right]. \tag{5.1}$$

Here all three terms are functions of the original $m+2$ momenta that enter the matrix element on the left hand side of eq. (5.1). To shorten the notation we denote these momenta collectively as $\{p\} \equiv \{p_1, \ldots, p_{m+2}\}$. Although the notation in eq. (5.1) is very similar to the operator notation introduced in ref. [47], it is important to understand that it is not meant in the operator sense, for instance, the last term on the right hand side does not refer to the collinear limit of anything. Throughout this paper the subtraction terms are functions of the original momenta for which the notation inherits the operator structure of taking the various limits, but otherwise it has nothing to do with taking limits.

5.1 Collinear counterterm

Counterterm. The singly-collinear counterterm is

$$\mathcal{C}^{(0,0)}_{ir}(\{p\}) = 8\pi\alpha_{\mathrm{s}}\mu^{2\varepsilon}\frac{1}{s_{ir}}\langle\mathcal{M}^{(0)}_{m+1}(\{\tilde{p}\}^{(ir)}_{m+1})|\hat{P}^{(0)}_{f_if_r}(z_{i,r}, z_{r,i}, k_{\perp,i,r};\varepsilon)|\mathcal{M}^{(0)}_{m+1}(\{\tilde{p}\}^{(ir)}_{m+1})\rangle\,, \tag{5.2}$$

where the kernels $\hat{P}^{(0)}_{f_if_r}(z_{i,r}, z_{r,i}, k_{\perp,i,r};\varepsilon)$ are defined to coincide with the following specific forms of the Altarelli-Parisi splitting functions (valid in the CDR scheme)

$$\langle r|\hat{P}^{(0)}_{q_ig_r}(z_{i,r}, z_{r,i};\varepsilon)|s\rangle = \delta_{rs}C_{\mathrm{F}}\left[\frac{1+z^2_{i,r}}{z_{r,i}} - \varepsilon z_{r,i}\right] \equiv \delta_{rs}P^{(0)}_{q_ig_r}(z_{i,r}, z_{r,i};\varepsilon)\,, \tag{5.3}$$

$$\langle\mu|\hat{P}^{(0)}_{\bar{q}_iq_r}(z_{i,r}, z_{r,i}, k^\mu_{\perp,i,r};\varepsilon)|\nu\rangle = T_{\mathrm{R}}\left[-g^{\mu\nu} + 4z_{i,r}z_{r,i}\frac{k^\mu_{\perp,i,r}k^\nu_{\perp,i,r}}{k^2_{\perp,i,r}}\right], \tag{5.4}$$

$$\langle\mu|\hat{P}^{(0)}_{g_ig_r}(z_{i,r}, z_{r,i}, k^\mu_{\perp,i,r};\varepsilon)|\nu\rangle = 2C_{\mathrm{A}}\left[-g^{\mu\nu}\left(\frac{z_{i,r}}{z_{r,i}} + \frac{z_{r,i}}{z_{i,r}}\right) - 2(1-\varepsilon)z_{i,r}z_{r,i}\frac{k^\mu_{\perp,i,r}k^\nu_{\perp,i,r}}{k^2_{\perp,i,r}}\right]. \tag{5.5}$$

In eq. (5.2) the double superscipt on the left hand side means that on the right hand side of the equation both the matrix elements as well as the splitting kernels are at tree-level.

In eq. (5.3) we introduced our notation for the spin-averaged splitting function,

$$P^{(0)}_{f_i f_r}(z_{i,r}, z_{r,i}; \varepsilon) \equiv \langle \hat{P}^{(0)}_{f_i f_r}(z_{i,r}, z_{r,i}, k^\mu_{\perp,i,r}; \varepsilon) \rangle \,. \tag{5.6}$$

The kernels are functions of the momentum fractions $z_{i,r}$ and $z_{r,i}$ that we define as

$$z_{i,r} = \frac{y_{iQ}}{y_{(ir)Q}} \qquad \text{and} \qquad z_{r,i} = \frac{y_{rQ}}{y_{(ir)Q}} \,, \tag{5.7}$$

where $y_{(ir)Q} = y_{iQ} + y_{rQ}$ with $y_{iQ} = 2p_i \cdot Q/Q^2$, $y_{rQ} = 2p_r \cdot Q/Q^2$ and Q^μ is the total four-momentum of the incoming electron and positron. With this definition $z_{i,r} + z_{r,i} = 1$. Note that the momentum fractions are nothing but the energy fractions of the daughter momenta of the splitting with respect to the energy of the parent parton in the center-of-momentum frame. The transverse momentum $k_{\perp,i,r}$ is given by

$$k^\mu_{\perp,i,r} = \zeta_{i,r} p^\mu_r - \zeta_{r,i} p^\mu_i + \zeta_{ir} \tilde{p}^\mu_{ir} \,, \qquad \zeta_{i,r} = z_{i,r} - \frac{y_{ir}}{\alpha_{ir} y_{(ir)Q}} \,, \quad \zeta_{r,i} = z_{r,i} - \frac{y_{ir}}{\alpha_{ir} y_{(ir)Q}} \,. \tag{5.8}$$

Here $y_{ir} = 2p_i \cdot p_r/Q^2$ while $\tilde{p}^\mu_{ir}$ and α_{ir} are defined below in eqs. (5.11) and (5.12) respectively. This choice for the transverse momentum is exactly perpendicular to the parent momentum $\tilde{p}^\mu_{ir}$ and ensures that in the collinear limit $p^\mu_i || p^\mu_r$, the square of $k^\mu_{\perp,i,r}$ behaves as

$$k^2_{\perp,i,r} \simeq -s_{ir} z_{r,i} z_{i,r} \,, \tag{5.9}$$

as required (independently of ζ_{ir}). In a NLO computation this feature is sufficient to ensure the correct collinear behaviour of the subtraction term. In a NNLO computation in addition to eq. (5.9) it is also important that $k^\mu_{\perp,i,r}$ itself vanishes in the collinear limit,[3] and it is convenient if $k^\mu_{\perp,i,r}$ is perpendicular to Q^μ. These conditions are fulfilled if we choose

$$\zeta_{ir} = \frac{y_{ir}}{\alpha_{ir} y_{\widetilde{ir}\,Q}} (z_{r,i} - z_{i,r}) \,. \tag{5.10}$$

With this choice $k^\mu_{\perp,i,r} \to k^\mu_{\perp,i}$ in the collinear limit as can be shown by substituting the Sudakov parametrization of the momenta into eq. (5.8) (with properly chosen gauge vector).

Momentum mapping and phase space factorization. The $m+1$ momenta, $\{\tilde{p}\}^{(ir)}_{m+1} \equiv \{\tilde{p}_1, \ldots, \tilde{p}_{ir}, \ldots, \tilde{p}_{m+2}\}$, entering the matrix elements on the right hand side of eq. (5.2) are defined as follows

$$\tilde{p}^\mu_{ir} = \frac{1}{1-\alpha_{ir}} (p^\mu_i + p^\mu_r - \alpha_{ir} Q^\mu) \,, \qquad \tilde{p}^\mu_n = \frac{1}{1-\alpha_{ir}} p^\mu_n \,, \qquad n \neq i, r \,, \tag{5.11}$$

where

$$\alpha_{ir} = \frac{1}{2} \left[y_{(ir)Q} - \sqrt{y^2_{(ir)Q} - 4 y_{ir}} \right] . \tag{5.12}$$

The total four-momentum is clearly conserved,

$$Q^\mu = p^\mu_i + p^\mu_r + \sum_n^m p^\mu_n = \tilde{p}^\mu_{ir} + \sum_n^m \tilde{p}^\mu_n \,. \tag{5.13}$$

[3] If $k^\mu_{\perp,i,r}$ does not vanish in the collinear limit then the iterated collinear-triple collinear counterterms of section 7.1 do not have the correct (strongly-ordered) collinear behaviour.

For further convenience let us denote the momentum mapping introduced above as

$$\{p\} \xrightarrow{\mathsf{C}_{ir}} \{\tilde{p}\}^{(ir)}_{m+1}\,, \tag{5.14}$$

where i and r are any two labels of momenta that appear on the left hand side, but not on the right hand side.

The momentum mapping of eq. (5.11) leads to exact phase space factorization in the form

$$\mathrm{d}\phi_{m+2}(\{p\};Q) = \mathrm{d}\phi_{m+1}(\{\tilde{p}\}^{(ir)}_{m+1};Q)\,[\mathrm{d}p^{(ir)}_{1;m+1}(p_r,\tilde{p}_{ir};Q)]\,, \tag{5.15}$$

where, as indicated, the $m+1$ momenta in the first factor on the right hand side of eq. (5.15) are exactly those defined in eq. (5.11). The explicit expression for $[\mathrm{d}p^{(ir)}_{1;m+1}(p_r,\tilde{p}_{ir};Q)]$ reads

$$[\mathrm{d}p^{(ir)}_{1;m+1}(p_r,\tilde{p}_{ir};Q)] = \mathcal{J}^{(ir)}_{1;m+1}(p_r,\tilde{p}_{ir};Q)\,\frac{\mathrm{d}^d p_r}{(2\pi)^{d-1}}\delta_+(p_r^2)\,, \tag{5.16}$$

where the Jacobian is

$$\mathcal{J}^{(ir)}_{1;m+1}(p_r,\tilde{p}_{ir};Q) = y_{\widetilde{ir}\,Q}\,\frac{(1-\alpha_{ir})^{m(d-2)-1}\,\Theta(1-\alpha_{ir})}{2(1-y_{\widetilde{ir}\,Q})\alpha_{ir} + y_{r\,\widetilde{ir}} + y_{\widetilde{ir}\,Q} - y_{rQ}}\,. \tag{5.17}$$

In this equation α_{ir} needs to be expressed as a function of the variables p_r^μ and $\tilde{p}_{ir}^\mu$, that is, it is the physical (falling between 0 and 1) solution of the constraint

$$\frac{p_i^2}{Q^2} = (1-y_{\widetilde{ir}\,Q})\,\alpha_{ir}^2 + (y_{r\,\widetilde{ir}} + y_{\widetilde{ir}\,Q} - y_{rQ})\,\alpha_{ir} - y_{r\,\widetilde{ir}} = 0\,, \tag{5.18}$$

which can be computed easily. However, for the purpose of defining the subtraction terms, this solution is not required explicitly, the momentum mapping given in eq. (5.11) is sufficient.

The collinear momentum mapping of eq. (5.11) and the implied phase-space factorization of eqs. (5.15)–(5.17) are represented graphically in figure 1. The leftmost picture represents the $(m+2)$-parton phase space $\mathrm{d}\phi_{m+2}(\{p\};Q)$. In the circle we denote the number of final-state partons. The picture in the middle represents the result of the mapping of momenta in eq. (5.11). The dots between the momentum $\tilde{p}_{ir}$ and the circle with the two momenta p_i and p_r means that the latter two are replaced with $\tilde{p}_{ir}$. This mapping implies the exact factorization of the phase space, written in eq. (5.15) and represented by the picture on the right. The first factor is the phase space of $(m+1)$-partons, $\mathrm{d}\phi_{m+1}(\{\tilde{p}\}^{(ir)}_{m+1};Q)$, and the second is $[\mathrm{d}p_1^{(ir)}]$. In the latter the box represents the Jacobian on eq. (5.17) and the line means the one-particle phase-space measure. We shall use similar graphical representations of other momentum mappings and implied factorizations of the phase space.

In the collinear limit, when $p_i^\mu || p_r^\mu$, the transverse momentum behaves as in eq. (5.9), $z_{i,r} \to z_i$ and $z_{r,i} \to z_r$. Furthermore, α_{ir} tends to zero so $\tilde{p}_{ir}^\mu \to p_i^\mu + p_r^\mu$ and $\tilde{p}_n \to p_n$, i.e. the tildes disappear from figure 1. Consequently, the counterterm reproduces the collinear behaviour of the squared matrix element in this limit.

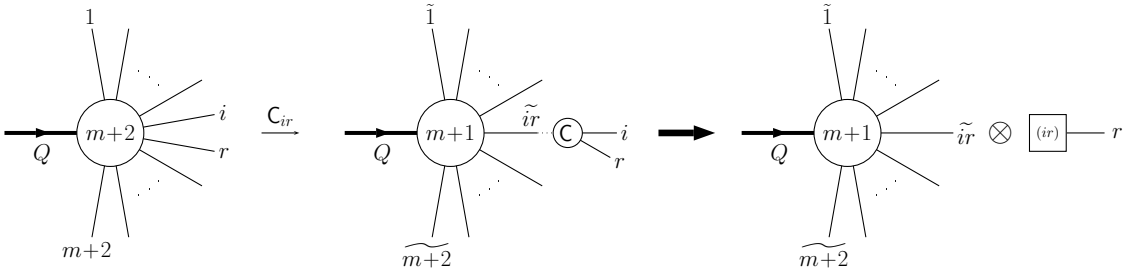

Figure 1: Graphical representation of the singly-collinear momentum mapping and the implied factorization of the phase space.

5.2 Soft-type counterterms

Counterterms. The soft-type[4] terms are the singly-soft and singly soft-collinear counterterms

$$\mathcal{S}^{(0,0)}_{r_g}(\{p\}) = -8\pi\alpha_{\rm s}\mu^{2\varepsilon}\sum_i\sum_{k\neq i}\frac{1}{2}\mathcal{S}_{ik}(r)|\mathcal{M}^{(0)}_{m+1,(i,k)}(\{\tilde{p}\}^{(r)}_{m+1})|^2\,, \tag{5.19}$$

$$\mathcal{C}_{ir_g}\mathcal{S}^{(0,0)}_{r_g}(\{p\}) = 8\pi\alpha_{\rm s}\mu^{2\varepsilon}\frac{1}{s_{ir}}\frac{2z_{i,r}}{z_{r,i}}\boldsymbol{T}_i^2\,|\mathcal{M}^{(0)}_{m+1}(\{\tilde{p}\}^{(r)}_{m+1})|^2\,. \tag{5.20}$$

If r is a quark or antiquark, $\mathcal{S}^{(0,0)}_{r}(\{p\})$ and $\mathcal{C}_{ir}\mathcal{S}^{(0,0)}_{r}(\{p\})$ are both zero. The eikonal factor in eq. (5.19) is

$$\mathcal{S}_{ik}(r) = \frac{2s_{ik}}{s_{ir}s_{rk}}\,, \tag{5.21}$$

and the momentum fractions entering eq. (5.20) are given in eq. (5.7). The operator $\boldsymbol{T}_i$ is the colour charge of parton i [6]. The matrix element, appearing in eq. (5.19) is the colour correlated squared matrix element (for the precise definition we refer to ref. [47]).

Momentum mapping and phase space factorization. The $m+1$ momenta, $\{\tilde{p}\}^{(r)}_{m+1} \equiv \{\tilde{p}_1,\ldots,\tilde{p}_{r-1},\tilde{p}_{r+1},\ldots,\tilde{p}_{m+2}\}$ (the momentum with index r is absent), entering the matrix elements on the right hand sides of eqs. (5.19) and (5.20) are defined by first rescaling all the hard momenta by a factor $1/\lambda_r$ and then transforming all of the rescaled momenta as

$$\tilde{p}^\mu_n = \Lambda^\mu_\nu[Q,(Q-p_r)/\lambda_r](p^\nu_n/\lambda_r)\,, \qquad n\neq r\,, \tag{5.22}$$

where

$$\lambda_r = \sqrt{1-y_{rQ}}\,, \tag{5.23}$$

and

$$\Lambda^\mu_\nu[K,\widetilde{K}] = g^\mu_\nu - \frac{2(K+\widetilde{K})^\mu(K+\widetilde{K})_\nu}{(K+\widetilde{K})^2} + \frac{2K^\mu\widetilde{K}_\nu}{K^2}\,. \tag{5.24}$$

[4]The expression 'soft-type' refers to the momentum mapping used to define these terms.

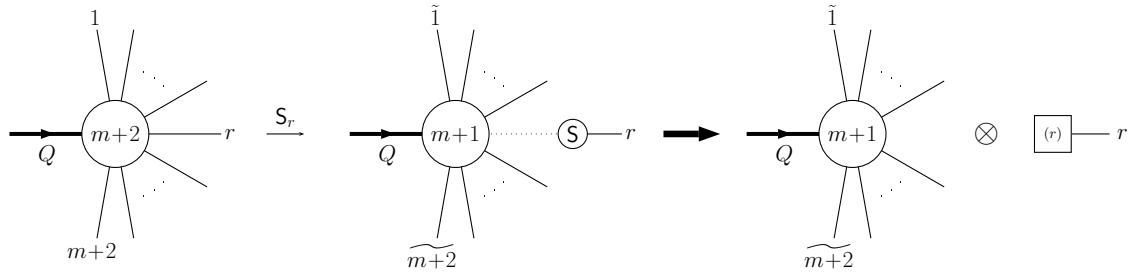

Figure 2: Graphical representation of the singly-soft momentum mapping and the implied factorization of the phase space.

The matrix $\Lambda^\mu_\nu[K, \widetilde{K}]$ generates a (proper) Lorentz transformation, provided $K^2 = \widetilde{K}^2 \neq 0$. Since p_r^μ is massless ($p_r^2 = 0$), the total four-momentum is again conserved,

$$Q^\mu = p_r^\mu + \sum_n^{m+1} p_n^\mu = \sum_n^{m+1} \tilde{p}_n^\mu \,. \tag{5.25}$$

We will find it convenient to introduce the notation

$$\{p\} \xrightarrow{\mathsf{S}_r} \{\tilde{p}\}^{(r)}_{m+1} \tag{5.26}$$

to denote the above momentum mapping. Here r is the label of any momentum of the original momentum set $\{p\}$ that is absent from the set on the right hand side.

The momentum mapping of eq. (5.22) also leads to exact phase space factorization

$$\mathrm{d}\phi_{m+2}(\{p\}; Q) = \mathrm{d}\phi_{m+1}(\{\tilde{p}\}^{(r)}_{m+1}; Q)\, [\mathrm{d}p^{(r)}_{1;m+1}(p_r; Q)] \,. \tag{5.27}$$

The $m+1$ momenta in the first factor on the right hand side are those of eq. (5.22). The factorized one-parton phase space $[\mathrm{d}p^{(r)}_{1;m+1}(p_r; Q)]$ is

$$[\mathrm{d}p^{(r)}_{1;m+1}(p_r; Q)] = \mathcal{J}^{(r)}_{1;m+1}(p_r; Q)\, \frac{\mathrm{d}^d p_r}{(2\pi)^{d-1}} \delta_+(p_r^2) \,, \tag{5.28}$$

with Jacobian

$$\mathcal{J}^{(r)}_{1;m+1}(p_r; Q) = \lambda_r^{m(d-2)-2} \Theta(\lambda_r) \,. \tag{5.29}$$

Similarly to the graphical representation of the collinear momentum mapping and phase-space factorization, depicted in figure 1, we present the graphical representation of eqs. (5.22)–(5.29) in figure 2. The middle picture in this figure represents the soft-type mapping of eq. (5.22). The dots between the main circle and the circle with momentum p_r mean that the latter does not take away momentum from Q^μ (see eq. (5.25)).

The soft-type terms are defined on the same phase space, therefore, in the collinear limit, when $p_i^\mu || p_r^\mu$, the soft-collinear counterterm regularizes the kinematical singularity of the soft counterterm by construction. In the soft limit, when $p_r^\mu \to 0$, in eqs. (5.11) and (5.12) $\alpha_{ir} \to 0$ and $\tilde{p}_{ir}^\mu \to p_i^\mu$, therefore, the momenta obtained in the collinear mapping tend to the same momenta as those obtained in the soft mapping, i.e. all momenta

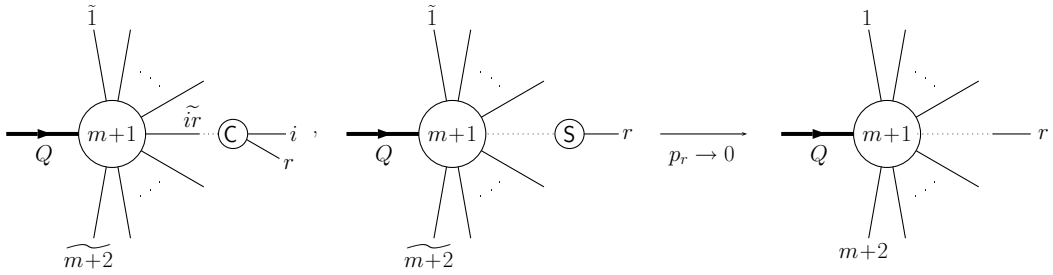

Figure 3: Graphical representation of the soft limit of collinear and soft-type mappings.

with tilde tend to the corresponding original momenta both in the case of collinear and soft momentum mappings, with the soft momentum being dropped as shown in figure 3. Thus the soft-collinear counterterm regularizes the kinematical singularity of the collinear counterterm. At the same time the soft one regularizes the squared matrix element by construction.

In closing this section, we note that the jet function J_{m+1} that multiplies $\mathrm{d}\sigma^{\mathrm{RR,A_1}}_{m+2}$ in eq. (3.3) is a function of the $m+1$ momenta $\{\tilde{p}\}^{(ir)}_{m+1}$ and $\{\tilde{p}\}^{(r)}_{m+1}$ for the collinear and soft-type countertems, respectively.

6. Doubly-unresolved counterterms

The doubly-unresolved counterterm is

$$\begin{aligned}\boldsymbol{\mathcal{A}}_2|\mathcal{M}^{(0)}_{m+2}|^2 = \sum_r\sum_{s\neq r}\Bigg\{\sum_{i\neq r,s}\Bigg[&\frac{1}{6}\mathcal{C}^{(0,0)}_{irs}(\{p\}) + \sum_{j\neq i,r,s}\frac{1}{8}\mathcal{C}^{(0,0)}_{ir;js}(\{p\})\\ &+\frac{1}{2}\left(\mathcal{CS}^{(0,0)}_{ir;s}(\{p\}) - \mathcal{C}_{irs}\mathcal{CS}^{(0,0)}_{ir;s}(\{p\}) - \sum_{j\neq i,r,s}\mathcal{C}_{ir;js}\mathcal{CS}^{(0,0)}_{ir;s}(\{p\})\right)\\ &-\mathcal{CS}_{ir;s}\mathcal{S}^{(0,0)}_{rs}(\{p\}) - \frac{1}{2}\mathcal{C}_{irs}\mathcal{S}^{(0,0)}_{rs}(\{p\}) + \mathcal{C}_{irs}\mathcal{CS}_{ir;s}\mathcal{S}^{(0,0)}_{rs}(\{p\})\\ &+\sum_{j\neq i,r,s}\frac{1}{2}\mathcal{C}_{ir;js}\mathcal{S}^{(0,0)}_{rs}(\{p\})\Bigg] + \frac{1}{2}\mathcal{S}^{(0,0)}_{rs}(\{p\})\Bigg\}. \end{aligned} \tag{6.1}$$

6.1 Triple collinear counterterm

Counterterm. The triple collinear counterterm reads

$$\mathcal{C}^{(0,0)}_{irs}(\{p\}) = (8\pi\alpha_{\mathrm{s}}\mu^{2\varepsilon})^2\frac{1}{s^2_{irs}}\langle\mathcal{M}^{(0)}_m(\{\tilde{p}\}^{(irs)}_m)|\hat{P}_{f_if_rf_s}(\{z_{j,kl},s_{jk},k_{\perp,j,kl}\};\varepsilon)|\mathcal{M}^{(0)}_m(\{\tilde{p}\}^{(irs)}_m)\rangle\,. \tag{6.2}$$

The $\hat{P}_{f_if_rf_s}(\{z_{j,kl},s_{jk},k_{\perp,j,kl}\};\varepsilon)$ kernels are defined to be the specific forms of the triple parton splitting functions introduced in ref. [47], with one important modification: In the gluon splitting functions $\hat{P}_{g_iq_r\bar{q}_s}$ and $\hat{P}_{g_ig_rg_s}$,[5] the azimuth-dependent terms that depend on

[5]In the case of the $g\to ggg$ splitting, ref. [47] uses the original definition of ref. [37], not spelled out explicitly.

JHEP01(2007)070

the transverse momenta have always to be written in the form $k^\mu_{\perp,j}k^\nu_{\perp,k}/k_{\perp,j}\cdot k_{\perp,k}$ (k can be equal to j), otherwise the collinear behaviour of the counterterm cannot be matched with that of the single collinear counterterm in the singly-unresolved phase space region. The correct azimuth-dependence can be achieved by making use of the following identites:

$$k^\mu_{\perp,j}k^\nu_{\perp,j} = \Big(- z_j(1-z_j)s_{jkl} + z_j s_{kl}\Big)\frac{k^\mu_{\perp,j}k^\nu_{\perp,j}}{k^2_{\perp,j}}\,, \tag{6.3}$$

$$2\,k^\mu_{\perp,j}k^\nu_{\perp,k} = \Big(s_{jk} + 2\,z_j z_k s_{jkl} - z_i s_{j(ik)} - z_j s_{i(jk)}\Big)\frac{k^\mu_{\perp,j}k^\nu_{\perp,k}}{k_{\perp,j}\cdot k_{\perp,k}}\,, \tag{6.4}$$

where $\{k,l\} = \{i,r,s\}\setminus\{j\}$ and j can be i, r or s. Note that ref. [47] does not consider the splitting function for the case of final-state fermions with identical flavours. The reason is that it consists of two terms of the type of different flavours plus a third term corresponding to an interference contribution denoted by $\langle\hat{P}^{(\mathrm{id})}_{\bar{q}_1 q_2 q_3}\rangle$ in ref. [37]. The different flavour contributions were given in ref. [47], while the interference term can directly be taken from ref. [37] with the simple substitution of indices $1\to r$, $2\to s$ and $3\to i$ in order to match our notation. This latter term does not require any special care because it does not have a leading singularity in any of the singly-, or other doubly-unresolved regions of the phase space, apart from the triple collinear one.

The momentum fractions in eq. (6.2) are defined similarly as for the collinear case given in eq. (5.7)

$$z_{i,rs} = \frac{y_{iQ}}{y_{(irs)Q}}\,, \qquad z_{r,is} = \frac{y_{rQ}}{y_{(irs)Q}}\,, \qquad z_{s,ir} = \frac{y_{sQ}}{y_{(irs)Q}}\,, \tag{6.5}$$

with $z_{i,rs} + z_{r,is} + z_{s,ir} = 1$. The transverse momentum $k_{\perp,r,is}$ is

$$k^\mu_{\perp,r,is} = \zeta_{r,is}p^\mu_i - \zeta_{i,rs}p^\mu_r + \zeta_{r,is}p^\mu_s - \zeta_{s,ir}p^\mu_r + \zeta_{ris}\,\tilde{p}^\mu_{irs}\,, \tag{6.6}$$

where[6]

$$\zeta_{i,rs} = z_{i,rs} - \frac{y_{(rs)i}}{\alpha_{irs}\,y_{(irs)Q}}\,, \qquad \zeta_{ris} = \frac{y_{ir} - y_{rs} - 2z_{r,is}y_{irs}}{\alpha_{irs}\,y_{\widetilde{irs}\,Q}}\,. \tag{6.7}$$

The expression for $k_{\perp,s,ir}$ is obtained from eq. (6.6) by simply interchanging the indices r and s, while $k_{\perp,i,rs} = -k_{\perp,r,is} - k_{\perp,s,ir}$. Similarly, $\zeta_{r,is}$ and $\zeta_{s,ir}$ are obtained from $\zeta_{i,rs}$, while ζ_{irs} and ζ_{sir} from ζ_{ris} by interchanging the indices. We define $\tilde{p}^\mu_{irs}$ and α_{irs} in eqs. (6.9) and (6.10). This choice for the transverse momentum is also perpendicular to the parent momentum $\tilde{p}^\mu_{irs}$ as the one given in eq. (5.8) and it ensures also that in the triple collinear limit $p^\mu_i||p^\mu_r||p^\mu_s$, relations of the type (see ref. [37])

$$s_{rs} \simeq -z_{r,is}\,z_{s,ir}\left(\frac{k_{\perp,r,is}}{z_{r,is}} - \frac{k_{\perp,s,ir}}{z_{s,ir}}\right)^2\,, \tag{6.8}$$

as well as $k_{\perp,r,is}\to k_{\perp,r}$ are fulfilled. In a NNLO computation the longitudinal component in eq. (6.6) does not give any contribution due to gauge invariance, therefore, we may choose $\zeta_{ris} = 0$.

[6]Note that the indices of ζ_{ris} are ordered!

Momentum mapping and phase space factorization. The matrix elements on the right hand side of eq. (6.2) are evaluated with the m momenta $\{\tilde{p}\}_m^{(irs)} \equiv \{\tilde{p}_1, \ldots, \tilde{p}_{irs}, \ldots, \tilde{p}_{m+2}\}$ defined as

$$\tilde{p}^\mu_{irs} = \frac{1}{1-\alpha_{irs}}(p_i^\mu + p_r^\mu + p_s^\mu - \alpha_{irs} Q^\mu)\,, \qquad \tilde{p}^\mu_n = \frac{1}{1-\alpha_{irs}} p_n^\mu\,, \qquad n \neq i,r,s\,, \tag{6.9}$$

with

$$\alpha_{irs} = \frac{1}{2}\left[y_{(irs)Q} - \sqrt{y^2_{(irs)Q} - 4y_{irs}}\,\right]. \tag{6.10}$$

Clearly eqs. (6.9) and (6.10) are generalizations of eqs. (5.11) and (5.12). The total four-momentum is again conserved,

$$Q^\mu = \tilde{p}^\mu_{irs} + \sum_n \tilde{p}^\mu_n = p_i^\mu + p_r^\mu + p_s^\mu + \sum_n p_n^\mu\,. \tag{6.11}$$

The momentum mapping of eq. (6.9) leads to exact phase-space factorization in a form very similar to eq. (5.15)

$$\mathrm{d}\phi_{m+2}(\{p\}; Q) = \mathrm{d}\phi_m(\{\tilde{p}\}_m^{(irs)}; Q)\,[\mathrm{d}p_{2;m}^{(irs)}(p_r, p_s, \tilde{p}_{irs}; Q)]\,, \tag{6.12}$$

where the m momenta in the first factor on the right hand side of eq. (6.12) are those given in eq. (6.9). The explicit expression for $[\mathrm{d}p_{2;m}^{(irs)}(p_r, p_s, \tilde{p}_{irs}; Q)]$ is

$$[\mathrm{d}p_{2;m}^{(irs)}(p_r, p_s, \tilde{p}_{irs}; Q)] = \mathcal{J}_{2;m}^{(irs)}(p_r, p_s, \tilde{p}_{irs}; Q)\,\frac{\mathrm{d}^d p_r}{(2\pi)^{d-1}}\delta_+(p_r^2)\,\frac{\mathrm{d}^d p_s}{(2\pi)^{d-1}}\delta_+(p_s^2)\,, \tag{6.13}$$

where the Jacobian is

$$\mathcal{J}_{2;m}^{(irs)}(p_r, p_s, \tilde{p}_{irs}; Q) = y_{\widetilde{irs}\,Q}\,\frac{(1-\alpha_{irs})^{(m-1)(d-2)-1}\,\Theta(1-\alpha_{irs})}{2(1-y_{\widetilde{irs}\,Q})\alpha_{irs} + y_{(rs)\,\widetilde{irs}} + y_{\widetilde{irs}\,Q} - y_{(rs)Q}}\,. \tag{6.14}$$

In this equation α_{irs} is the physical (falling between 0 and 1) solution of the constraint

$$\frac{p_i^2}{Q^2} = (1 - y_{\widetilde{irs}\,Q})\,\alpha_{irs}^2 + (y_{(rs)\,\widetilde{irs}} + y_{\widetilde{irs}\,Q} - y_{(rs)Q})\,\alpha_{irs} + y_{rs} - y_{(rs)\,\widetilde{irs}} = 0\,. \tag{6.15}$$

We present the graphical representation of eqs. (6.9)–(6.14) in figure 4. The meaning of the various graphical elements is analogous to those in figure 1.

In the triply-collinear limit, when $p_i^\mu || p_r^\mu || p_s^\mu$, the transverse momenta behave as in eq. (6.8), $z_{i,rs} \to z_i$, $z_{r,is} \to z_r$ and $z_{s,ir} \to z_s$. Furthermore, α_{irs} tends to zero so $\tilde{p}^\mu_{irs} \to p_i^\mu + p_r^\mu + p_s^\mu$ and $\tilde{p}_n \to p_n$ (the tildes disappear from figure 4). Consequently, the counterterm reproduces the collinear behaviour of the squared matrix element in this limit.

6.2 Double collinear counterterm

Counterterm. The double collinear subtraction term reads

$$\mathcal{C}^{(0,0)}_{ir;js}(\{p\}) = (8\pi\alpha_{\mathrm{s}}\mu^{2\varepsilon})^2 \frac{1}{s_{ir}s_{js}} \tag{6.16}$$
$$\times \langle \mathcal{M}_m^{(0)}(\{\tilde{p}\}_m^{(ir;js)})|\hat{P}^{(0)}_{f_i f_r}(z_{i,r}, z_{r,i}, k_{\perp,ir;js}; \varepsilon)\hat{P}^{(0)}_{f_j f_s}(z_{j,s}, z_{s,j}, k_{\perp,js;ir}; \varepsilon)|\mathcal{M}_m^{(0)}(\{\tilde{p}\}_m^{(ir;js)})\rangle\,,$$

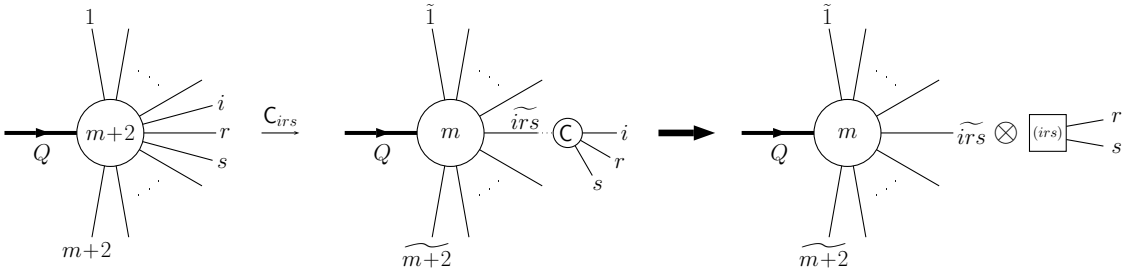

Figure 4: Graphical representation of the triply-collinear momentum mapping and the implied factorization of the phase space.

where $\hat{P}^{(0)}_{f_k f_l}(z_k, z_l, k_\perp; \varepsilon)$ are given in eqs. (5.3)–(5.5). The momentum fractions are defined in eq. (5.7), and the transverse momentum $k_{\perp,ir;js}$ is

$$k^\mu_{\perp,ir;js} = \zeta_{i,r} p^\mu_r - \zeta_{r,i} p^\mu_i + \zeta_{ir} \tilde{p}^\mu_{ir}\,, \tag{6.17}$$

i.e., it is formally identical to the $k^\mu_{\perp,i,r}$ defined in eq. (5.8), although the definition of $\tilde{p}^\mu_{ir}$ is different in the two cases (cf. eqs. (5.11) and (6.18)). In the NNLO computation we may choose $\zeta_{ir} = 0$ in eq. (6.17). Of course, $k_{\perp,js;ir}$ is given by eq. (6.17) after the interchange of indices ($i \leftrightarrow j, r \leftrightarrow s$). Eq. (5.12) defines α_{ir} and α_{js}, the latter with the same change of indices as before.

Momentum mapping and phase space factorization. The m momenta $\{\tilde{p}\}^{(ir;js)}_m \equiv \{\tilde{p}, \ldots, \tilde{p}_{ir}, \ldots, \tilde{p}_{js}, \ldots, \tilde{p}_{m+2}\}$ entering the matrix element on the right hand side of eq. (6.16) are again given by a simple generalization of eq. (5.11)

$$\tilde{p}^\mu_{ir} = \frac{1}{1-\alpha_{ir}-\alpha_{js}}(p^\mu_i + p^\mu_r - \alpha_{ir} Q^\mu)\,, \qquad \tilde{p}^\mu_{js} = \frac{1}{1-\alpha_{ir}-\alpha_{js}}(p^\mu_j + p^\mu_s - \alpha_{js} Q^\mu)\,,$$
$$\tilde{p}^\mu_n = \frac{1}{1-\alpha_{ir}-\alpha_{js}} p^\mu_n\,, \qquad n \neq i, r, j, s\,. \tag{6.18}$$

The total four-momentum is clearly conserved.

The momentum mapping of eq. (6.18) leads to the following exact factorization of the phase space:

$$\mathrm{d}\phi_{m+2}(\{p\}; Q) = \mathrm{d}\phi_m(\{\tilde{p}\}^{(ir;js)}_m; Q)\, [\mathrm{d}p^{(ir;js)}_{2;m}(p_r, p_s, \tilde{p}_{ir}, \tilde{p}_{js}; Q)]\,. \tag{6.19}$$

where the m momenta in the first factor on the right hand side of eq. (6.19) are given by eq. (6.18) and $[\mathrm{d}p^{(ir;js)}_{2;m}(p_r, p_s, \tilde{p}_{ir}, \tilde{p}_{js}; Q)]$ reads

$$[\mathrm{d}p^{(ir;js)}_{2;m}(p_r, p_s, \tilde{p}_{ir}, \tilde{p}_{js}; Q)] = \mathcal{J}^{(ir;js)}_{2;m}(p_r, p_s, \tilde{p}_{ir}, \tilde{p}_{js}; Q) \frac{\mathrm{d}^d p_r}{(2\pi)^{d-1}} \delta_+(p_r^2)\, \frac{\mathrm{d}^d p_s}{(2\pi)^{d-1}} \delta_+(p_s^2)\,. \tag{6.20}$$

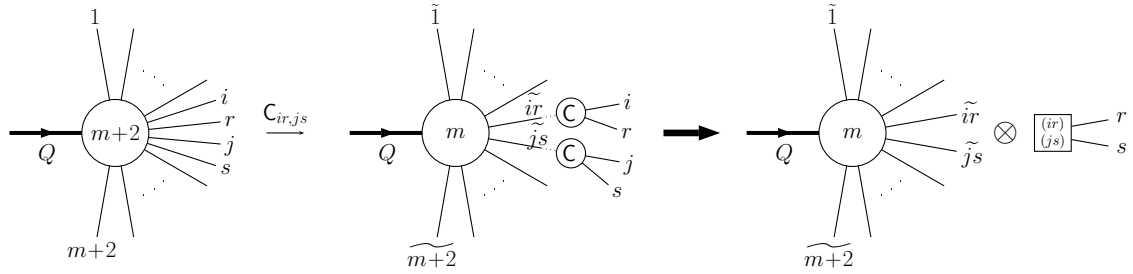

Figure 5: Graphical representation of the doubly-collinear momentum mapping and the implied factorization of the phase space.

In this equation the Jacobian factor can be written as, for instance,

$$\begin{aligned}\mathcal{J}^{(ir;js)}_{2;m}(p_r,p_s,\tilde{p}_{ir},\tilde{p}_{js};Q) &= y_{\widetilde{ir}\,Q}\,y_{\widetilde{js}\,Q}\,(1-\alpha_{ir}-\alpha_{js})^{(m-1)(d-2)}\,\Theta(1-\alpha_{ir}-\alpha_{js})\\ &\times\Bigg(4(1-y_{\widetilde{ir}\,Q}-y_{\widetilde{js}\,Q})\alpha_{ir}\alpha_{js}\\ &+\Big[y_{\widetilde{js}\,Q}(2-y_{\widetilde{ir}\,Q}+y_{r\,\widetilde{ir}}-y_{rQ})+y_{s\,\widetilde{js}}(2+y_{\widetilde{ir}\,Q})-2y_{sQ}(1-y_{\widetilde{ir}\,Q})\Big]\alpha_{ir}\\ &+\Big[y_{\widetilde{ir}\,Q}(2-y_{\widetilde{js}\,Q}+y_{s\,\widetilde{js}}-y_{sQ})+y_{r\,\widetilde{ir}}(2+y_{\widetilde{js}\,Q})-2y_{rQ}(1-y_{\widetilde{js}\,Q})\Big]\alpha_{js}\\ &+(y_{\widetilde{ir}\,Q}-y_{rQ})(y_{\widetilde{js}\,Q}-y_{sQ})-(y_{\widetilde{ir}\,Q}+y_{rQ})y_{s\,\widetilde{js}}-(y_{\widetilde{js}\,Q}+y_{sQ})y_{r\,\widetilde{ir}}\Bigg)^{-1}, \quad (6.21)\end{aligned}$$

where α_{ir} and α_{js} are the physical (both are positive and their sum falling between 0 and 1) solutions of the coupled constraints

$$\begin{aligned}\frac{p_i^2}{Q^2} &= (1-y_{\widetilde{ir}\,Q})\,\alpha_{ir}^2-y_{\widetilde{ir}\,Q}\,\alpha_{ir}\alpha_{js}+(y_{r\,\widetilde{ir}}+y_{\widetilde{ir}\,Q}-y_{rQ})\,\alpha_{ir}+y_{r\,\widetilde{ir}}\alpha_{js}-y_{r\,\widetilde{ir}}=0\,,\\ \frac{p_j^2}{Q^2} &= (1-y_{\widetilde{js}\,Q})\,\alpha_{js}^2-y_{\widetilde{js}\,Q}\,\alpha_{ir}\alpha_{js}+(y_{s\,\widetilde{js}}+y_{\widetilde{js}\,Q}-y_{sQ})\,\alpha_{js}+y_{s\,\widetilde{js}}\alpha_{is}-y_{s\,\widetilde{js}}=0\,. \quad (6.22)\end{aligned}$$

The analytical solution of these equations is rather complicated. In a numerical calculation one can always find the solution numerically. However, for defining the subtraction terms, we need only the momentum mapping given in eq. (6.18). In order to integrate the subtraction term over the factorized phase space $[\mathrm{d}p^{(ir;js)}_{2;m}(p_r,p_s,\tilde{p}_{ir},\tilde{p}_{js};Q)]$, we can choose α_{ir} and α_{js} as integration variables and thus the solution of the coupled quadratic equations can be avoided. We present the graphical representation of eqs. (6.18)–(6.21) in figure 5.

In the doubly-collinear limit, when $p_i^\mu||p_r^\mu$ and $p_j^\mu||p_s^\mu$, the transverse momenta behave as in eq. (5.9), $z_{k,l}\to z_k$ ($k,\ l=i,\ j,\ r,\ s$). Both α_{ir} and α_{js} tend to zero so $\tilde{p}^\mu_{ir}\to p_i^\mu+p_r^\mu$, $\tilde{p}^\mu_{js}\to p_j^\mu+p_s^\mu$, $\tilde{p}^\mu_n\to p_n^\mu$. Consequently, the counterterm properly regularizes the squared matrix element in this limit.

6.3 Double soft-collinear-type counterterms

Counterterms. We refer to the three terms on the second line of eq. (6.1) as double soft-collinear-type terms because they are all defined using the same momentum mapping,

that of the soft-collinear subtraction term. Explicitly these terms read

$$\begin{aligned}
\mathcal{CS}^{(0,0)}_{ir;s}(\{p\}) &= -(8\pi\alpha_{\rm s}\mu^{2\varepsilon})^2 \sum_j \sum_{k\neq j} \frac{1}{2}\mathcal{S}_{jk}(s) \\
&\quad \times \frac{1}{s_{ir}} \langle \mathcal{M}^{(0)}_m(\{\tilde{p}\}^{(\hat{s},ir)}_m) | \boldsymbol{T}_j \boldsymbol{T}_k \hat{P}^{(0)}_{f_i f_r}(z_{i,r}, z_{r,i}, \tilde{k}_{\perp,i,r}; \varepsilon) | \mathcal{M}^{(0)}_m(\{\tilde{p}\}^{(\hat{s},ir)}_m) \rangle , \qquad (6.23) \\
\mathcal{C}_{irs}\mathcal{CS}^{(0,0)}_{ir;s}(\{p\}) &= (8\pi\alpha_{\rm s}\mu^{2\varepsilon})^2 \frac{2}{s_{(ir)s}} \frac{1-z_{s,ir}}{z_{s,ir}} \boldsymbol{T}^2_{ir} \\
&\quad \times \frac{1}{s_{ir}} \langle \mathcal{M}^{(0)}_m(\{\tilde{p}\}^{(\hat{s},ir)}_m) | \hat{P}^{(0)}_{f_i f_r}(z_{i,r}, z_{r,i}, \tilde{k}_{\perp,i,r}; \varepsilon) | \mathcal{M}^{(0)}_m(\{\tilde{p}\}^{(\hat{s},ir)}_m) \rangle , \qquad (6.24) \\
\mathcal{C}_{ir;js}\mathcal{CS}^{(0,0)}_{ir;s}(\{p\}) &= (8\pi\alpha_{\rm s}\mu^{2\varepsilon})^2 \frac{2}{s_{js}} \frac{z_{j,s}}{z_{s,j}} \boldsymbol{T}^2_j \\
&\quad \times \frac{1}{s_{ir}} \langle \mathcal{M}^{(0)}_m(\{\tilde{p}\}^{(\hat{s},ir)}_m) | \hat{P}^{(0)}_{f_i f_r}(z_{i,r}, z_{r,i}, \tilde{k}_{\perp,i,r}; \varepsilon) | \mathcal{M}^{(0)}_m(\{\tilde{p}\}^{(\hat{s},ir)}_m) \rangle . \qquad (6.25)
\end{aligned}$$

Here we remind the reader of what we wrote below eq. (5.1) about the notation. For instance, on the left hand side of eq. (6.24) $\mathcal{C}_{irs}\mathcal{CS}^{(0,0)}_{ir;s}$ denotes a function that is defined by the function of the original momenta given on the right hand side. The eikonal factor entering the soft-collinear counterterm $\mathcal{CS}^{(0,0)}_{ir;s}(\{p\})$ is given in eq. (5.21). Nevertheless, we record explicitly that whenever j or l in eq. (6.23) is equal to (ir), eq. (5.21) evaluates to

$$\mathcal{S}_{(ir)l}(s) = \frac{2s_{(ir)l}}{s_{(ir)s}s_{ls}} = \frac{2(s_{il}+s_{rl})}{(s_{is}+s_{rs})s_{ls}} . \qquad (6.26)$$

The momentum fractions appearing in eqs. (6.23)–(6.25) are the same as those for the singly- and triply-collinear counterterm (see eq. (5.7) and eq. (6.5)), while transverse components $\tilde{k}_{\perp,i,r}$ are the image of the transverse momentum $k_{\perp,i,r}$ in eq. (5.8) under the soft map of eq. (5.26)

$$k_{\perp,i,r} \xrightarrow{\mathsf{S}_{\hat{s}}} \tilde{k}_{\perp,i,r} . \qquad (6.27)$$

Explicitly we have

$$\tilde{k}^{\mu}_{\perp,i,r} = \Lambda^{\mu}_{\nu}[Q, (Q-p_{\hat{s}})/\lambda_{\hat{s}}](k^{\nu}_{\perp,i,r}/\lambda_{\hat{s}}) , \qquad (6.28)$$

where $\lambda_{\hat{s}}$ and the matrix Λ^{μ}_{ν} are defined in eqs. (5.23) and (5.24). The hatted momentum $\hat{p}_s$ is given in eq. (6.30) with $n = s$.

Momentum mapping and phase space factorization. The m momenta $\{\tilde{p}\}^{(\hat{s},ir)}_m \equiv \{\tilde{p}_1, \ldots, \tilde{p}_{ir}, \ldots, \tilde{p}_{m+2}\}$ (p_s is absent) entering the matrix elements on the right hand sides of eqs. (6.23)–(6.25) are defined by the composition of a single collinear and a single soft mapping as follows:

$$\{p\} \xrightarrow{\mathsf{C}_{ir}} \{\hat{p}\}^{(ir)}_{m+1} \xrightarrow{\mathsf{S}_{\hat{s}}} \{\tilde{p}\}^{(\hat{s},ir)}_m . \qquad (6.29)$$

The first mapping is a collinear-type one leading to the hatted momenta

$$\hat{p}^{\mu}_{ir} = \frac{1}{1-\alpha_{ir}}(p^{\mu}_i + p^{\mu}_r - \alpha_{ir}Q^{\mu}) , \qquad \hat{p}^{\mu}_n = \frac{1}{1-\alpha_{ir}} p^{\mu}_n , \qquad n \neq i, r , \qquad (6.30)$$

where α_{ir} is given in eq. (5.12), followed by a soft mapping

$$\tilde{p}^{\mu}_n = \Lambda^{\mu}_{\nu}[Q, (Q-\hat{p}_s)/\lambda_{\hat{s}}](\hat{p}^{\nu}_n/\lambda_{\hat{s}}) , \qquad n \neq \hat{s} , \qquad (6.31)$$

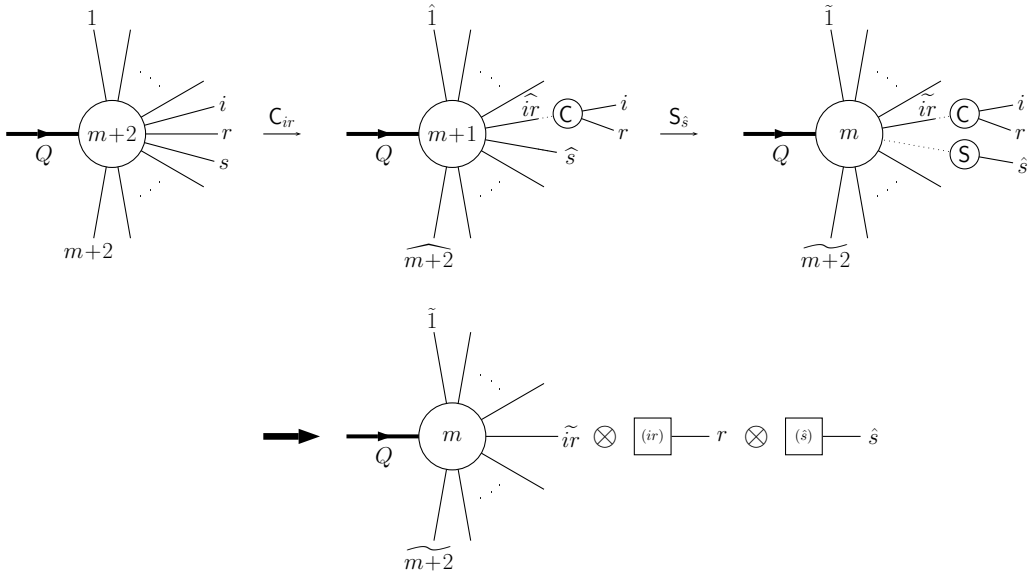

Figure 6: Graphical representation of the soft-collinear momentum mapping and the implied factorization of the phase space.

where $\lambda_{\hat{s}}$ is given in eq. (5.23) (with $r \to \hat{s}$). The order of the soft and collinear mappings is not crucial. The order chosen here leads to simpler integrals of the singular factors over the unresolved phase space.

This momentum mapping leads to exact phase-space factorization

$$\mathrm{d}\phi_{m+2}(\{p\};Q) = \mathrm{d}\phi_m(\{\tilde{p}\}_m^{(\hat{s},ir)};Q)\,[\mathrm{d}p_{1;m+1}^{(ir)}(p_r,\hat{p}_{ir};Q)]\,[\mathrm{d}p_{1;m}^{(\hat{s})}(\hat{p}_s;Q)]\,. \tag{6.32}$$

The collinear and soft one-particle factorized phase space measures $[\mathrm{d}p_{1;m+1}^{(ir)}(p_r,\hat{p}_{ir};Q)]$ and $[\mathrm{d}p_{1;m}^{(\hat{s})}(\hat{p}_s;Q)]$ are given respectively in eqs. (5.16) and (5.28). We show a graphical representation for eqs. (6.29)–(6.32) in figure 6. The counterterms in eqs. (6.23)–(6.25) are defined on the same phase spaces. Therefore, in the triply-collinear limit, when $p_i^\mu||p_r^\mu||p_s^\mu$, the term in eq. (6.24) regularizes that in eq. (6.23), while eq. (6.25) is integrable. Conversely, in the doubly-collinear limit, when $p_i^\mu||p_r^\mu$ and $p_j^\mu||p_s^\mu$, the term in eq. (6.25) regularizes that in eq. (6.23), while eq. (6.24) is integrable. In the soft-collinear limit, when $p_i^\mu||p_r^\mu$ and $p_s^\mu \to 0$ simultaneously, both the triply-collinear mapping, defined in eqs. (6.9) and (6.10), and the doubly-collinear mapping, defined in eq. (6.18), approach the corresponding limit of the iterated mappings of eqs. (6.29)–(6.31). This limit of the momentum mappings is depicted graphically in figure 7. We then conclude that the subtraction term in eq. (6.24) regularizes the kinematical singularities in eq. (6.2), while eq. (6.25) regularizes the singularities in the doubly-collinear subtraction in eq. (6.16). In this limit, the subtraction term in eq. (6.23) is a local counterterm to the squared matrix element by construction.

6.4 Double soft-type counterterms

All terms on the last two lines of eq. (6.1) are constructed using the same momentum mapping as the doubly soft counterterm $\mathcal{S}_{rs}^{(0,0)}(\{p\})$ itself. We refer to these as doubly soft-type terms.

JHEP01(2007)070

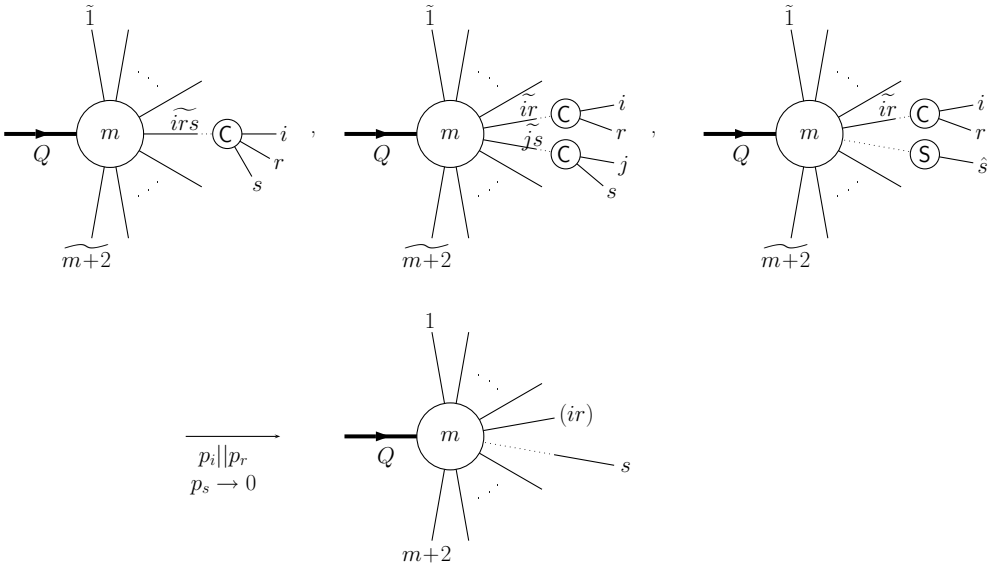

Figure 7: Graphical representation of the soft-collinear limit of the triply-, doubly- and soft-collinear momentum mappings.

Counterterms. We begin by exhibiting the soft-type terms explicitly for the case of double soft gluon emission and then present counterterms to it in the various doubly-unresolved regions. We have

$$\mathcal{S}^{(0,0)}_{r_g s_g}(\{p\}) = (8\pi\alpha_{\rm s}\mu^{2\varepsilon})^2 \left[\frac{1}{8}\sum_{i,j,k,l}\mathcal{S}_{ik}(r)\mathcal{S}_{jl}(s)|\mathcal{M}^{(0)}_{m;(i,k)(j,l)}(\{\tilde{p}\}^{(rs)}_m)|^2 - \frac{1}{4}C_{\rm A}\sum_{i,k}\mathcal{S}_{ik}(r,s)|\mathcal{M}^{(0)}_{m;(i,k)}(\{\tilde{p}\}^{(rs)}_m)|^2\right], \tag{6.33}$$

$$\begin{aligned}\mathcal{C}_{ir_g s_g}\mathcal{S}^{(0,0)}_{r_g s_g}(\{p\}) = (8\pi\alpha_{\rm s}\mu^{2\varepsilon})^2 \Bigg\{ & \boldsymbol{T}_i^2\,\frac{4z_{i,rs}^2}{s_{ir}s_{is}z_{r,is}z_{s,ir}} + C_{\rm A}\Bigg[\frac{(1-\varepsilon)}{s_{i(rs)}s_{rs}}\frac{(s_{ir}z_{s,ir}-s_{is}z_{r,is})^2}{s_{i(rs)}s_{rs}(z_{r,is}+z_{s,ir})^2} \\ & - \frac{z_{i,rs}}{s_{i(rs)}s_{rs}}\left(\frac{4}{z_{r,is}+z_{s,ir}}-\frac{1}{z_{r,is}}\right) - \frac{1}{s_{i(rs)}s_{ir}}\frac{2z_{i,rs}^2}{z_{r,is}(z_{r,is}+z_{s,ir})} \\ & - \frac{z_{i,rs}^2}{s_{i(rs)}s_{is}}\frac{1}{z_{r,is}(z_{r,is}+z_{s,ir})} + \frac{z_{i,rs}}{s_{ir}s_{rs}}\left(\frac{1}{z_{s,ir}}+\frac{1}{z_{r,is}+z_{s,ir}}\right) + (r\leftrightarrow s)\Bigg]\Bigg\} \\ & \times \boldsymbol{T}_i^2\,|\mathcal{M}^{(0)}_m(\{\tilde{p}\}^{(rs)}_m)|^2\,,\end{aligned} \tag{6.34}$$

$$\mathcal{CS}_{ir_g;s_g}\mathcal{S}^{(0,0)}_{r_g s_g}(\{p\}) = -(8\pi\alpha_{\rm s}\mu^{2\varepsilon})^2\frac{1}{s_{ir}}\frac{2z_{i,r}}{z_{r,i}}\boldsymbol{T}_i^2\sum_j\sum_{l\neq j}\frac{1}{2}\mathcal{S}_{jl}(s)|\mathcal{M}^{(0)}_{m;(j,l)}(\{\tilde{p}\}^{(rs)}_m)|^2\,, \tag{6.35}$$

$$\mathcal{C}_{ir_g;js_g}\mathcal{S}^{(0,0)}_{r_g s_g}(\{p\}) = (8\pi\alpha_{\rm s}\mu^{2\varepsilon})^2\frac{1}{s_{ir}}\frac{2z_{i,r}}{z_{r,i}}\boldsymbol{T}_i^2\frac{1}{s_{js}}\frac{2z_{j,s}}{z_{s,j}}\boldsymbol{T}_j^2|\mathcal{M}^{(0)}_m(\{\tilde{p}\}^{(rs)}_m)|^2\,, \tag{6.36}$$

$$\mathcal{C}_{ir_g s_g}\mathcal{CS}_{ir_g;s_g}\mathcal{S}^{(0,0)}_{r_g s_g} = (8\pi\alpha_{\rm s}\mu^{2\varepsilon})^2\frac{4z_{i,rs}(z_{i,rs}+z_{r,is})}{s_{ir}s_{(ir)s}z_{r,is}z_{s,ir}}\boldsymbol{T}_i^2\boldsymbol{T}_i^2|\mathcal{M}^{(0)}_m(\{\tilde{p}\}^{(rs)}_m)|^2\,. \tag{6.37}$$

The momentum fractions were defined in eqs. (5.7) and (6.5). The matrix elements, appearing in eq. (6.33) are the doubly two-parton colour-correlated squared matrix elements. For their precise definition we refer to ref. [47]. The two-gluon soft function appearing in eq. (6.33) is

$$\mathcal{S}_{ik}(r,s) = \mathcal{S}_{ik}^{(\mathrm{s.o.})}(r,s) + 4\frac{s_{ir}s_{ks}+s_{is}s_{kr}}{s_{i(rs)}s_{k(rs)}}\left[\frac{1-\varepsilon}{s_{rs}^2} - \frac{1}{8}\mathcal{S}_{ik}^{(\mathrm{s.o.})}(r,s)\right] - \frac{4}{s_{rs}}\mathcal{S}_{ik}(rs)\,, \tag{6.38}$$

where

$$\mathcal{S}_{ik}^{(\mathrm{s.o.})}(r,s) = \mathcal{S}_{ik}(s)\left(\mathcal{S}_{is}(r) + \mathcal{S}_{ks}(r) - \mathcal{S}_{ik}(r)\right) \tag{6.39}$$

is the form of this function in the strongly-ordered approximation and $\mathcal{S}_{ik}(rs)$ is given by eq. (5.21),

$$\mathcal{S}_{ik}(rs) = \frac{2s_{ik}}{s_{i(rs)}s_{k(rs)}}\,. \tag{6.40}$$

The discussion below eq. (6.25) about the eikonal factor appering in the double soft-collinear subtraction term (eq. (6.23)) and especially eq. (6.26) apply also to the soft-collinear limit of the doubly-soft subtraction, eq. (6.35).

The only nonzero terms for the case of emission of a soft quark-antiquark pair are $\mathcal{S}^{(0,0)}_{r_{\bar{q}}s_q}(\{p\})$ and $\mathcal{C}_{ir_{\bar{q}}s_q}\mathcal{S}^{(0,0)}_{r_{\bar{q}}s_q}(\{p\})$, the remaining terms all vanish. Explicit expressions for these nonzero terms are

$$\begin{aligned}\mathcal{S}^{(0,0)}_{r_{\bar{q}}s_q}(\{p\}) &= (8\pi\alpha_{\mathrm{s}}\mu^{2\varepsilon})^2\,\frac{1}{s_{rs}^2}\,T_{\mathrm{R}} \\ &\quad\times\sum_i\sum_{k\neq i}\left(\frac{s_{ir}s_{ks}+s_{kr}s_{is}-s_{ik}s_{rs}}{s_{i(rs)}s_{k(rs)}} - 2\frac{s_{ir}s_{is}}{s_{i(rs)}^2}\right)|\mathcal{M}^{(0)}_{m;(i,k)}(\{\tilde{p}\}_m^{(rs)})|^2,\end{aligned} \tag{6.41}$$

$$\begin{aligned}\mathcal{C}_{ir_{\bar{q}}s_q}\mathcal{S}^{(0,0)}_{r_{\bar{q}}s_q}(\{p\}) &= (8\pi\alpha_{\mathrm{s}}\mu^{2\varepsilon})^2\,\boldsymbol{T}_i^2\,T_{\mathrm{R}} \\ &\quad\times\frac{2}{s_{i(rs)}s_{rs}}\left(\frac{z_{i,rs}}{z_{r,is}+z_{s,ir}} - \frac{(s_{ir}z_{s,ir}-s_{is}z_{r,is})^2}{s_{i(rs)}s_{rs}(z_{r,is}+z_{s,ir})^2}\right)|\mathcal{M}^{(0)}_{m}(\{\tilde{p}\}_m^{(rs)})|^2.\end{aligned} \tag{6.42}$$

Momentum mapping and phase space factorization. The m momenta $\{\tilde{p}\}_m^{(rs)} \equiv \{\tilde{p}_1,\ldots,\tilde{p}_{m+2}\}$ (p_r and p_s are omitted from the set) entering the matrix elements on the right hand sides of eqs. (6.33)–(6.37) and eqs. (6.41) and (6.42) are given by a generalization of the singly-soft momentum mapping of eq. (5.22) to the case of two soft momenta,

$$\tilde{p}_n^\mu = \Lambda^\mu_\nu[Q,(Q-p_r-p_s)/\lambda_{rs}](p_n^\nu/\lambda_{rs})\,, \qquad n\neq r,s\,, \tag{6.43}$$

where

$$\lambda_{rs} = \sqrt{1-\left(y_{(rs)Q}-y_{rs}\right)} \tag{6.44}$$

and $\Lambda^\mu_\nu[Q,(Q-p_r-p_s)/\lambda_{rs}]$ is the matrix given in eq. (5.24). This momentum mapping again conserves total four-momentum.

The $m+2$ parton phase space factorizes exactly under the mapping of eq. (6.43). We find

$$\mathrm{d}\phi_{m+2}(\{p\};Q) = \mathrm{d}\phi_m(\{\tilde{p}\}_m^{(rs)};Q)[\mathrm{d}p_{2;m}^{(rs)}(p_r,p_s;Q)]\,, \tag{6.45}$$

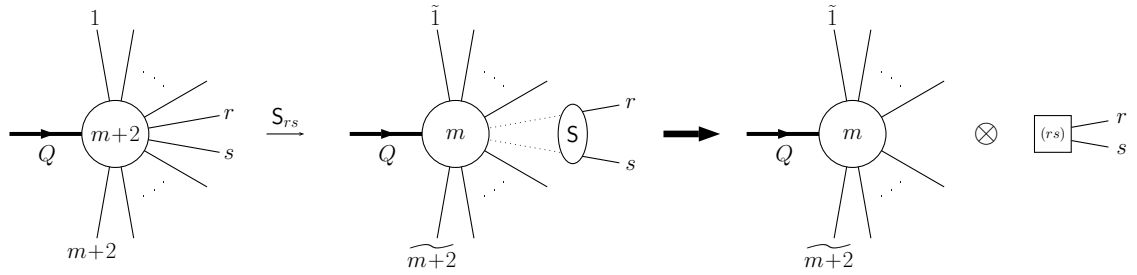

Figure 8: Graphical representation of the doubly-soft momentum mapping and the implied factorization of the phase space.

where the m momenta in the first factor on the right hand side are those defined in eq. (6.43). The explicit form of the factorized two-parton phase space is

$$[\mathrm{d}p^{(rs)}_{2;m}(p_r,p_s;Q)] = \mathcal{J}^{(rs)}_{2;m}(p_r,p_s;Q)\,\frac{\mathrm{d}^d p_r}{(2\pi)^{d-1}}\delta_+(p_r^2)\,\frac{\mathrm{d}^d p_s}{(2\pi)^{d-1}}\delta_+(p_s^2)\,, \tag{6.46}$$

with Jacobian

$$\mathcal{J}^{(rs)}_{2;m}(p_r,p_s;Q) = \lambda_{rs}^{m(d-2)-2}\Theta(\lambda_{rs})\,. \tag{6.47}$$

We show a graphical representation for eqs. (6.43)–(6.47) in figure 8.

The counterterms in eqs. (6.33)–(6.37) are all defined on the same phase spaces. Therefore, all the cancellations among these terms in the triply-collinear limit, when $p_i^\mu||p_r^\mu||p_s^\mu$, in the doubly-collinear limit, when $p_i^\mu||p_r^\mu$ and $p_j^\mu||p_s^\mu$, and in the soft-collinear limit, when $p_i^\mu||p_r^\mu$ and $p_s^\mu\to 0$, take place in just the same way as for the QCD factorization formulae described in ref. [47]. Consequently, the combination of the terms in eqs. (6.33)–(6.37) as present in eq. (6.1) is integrable in four dimensions in all of these limits. The same is true for the difference of the two terms in eqs. (6.41) and (6.42).

In the doubly-soft regions of the phase space, when p_r^μ and $p_s^\mu\to 0$, the momentum mappings in eqs. (6.9), (6.18) and in (6.29) approach the corresponding limit of the double soft-type mapping in eq. (6.43), shown graphically in figure 9. Therefore, the cancellation of kinematical singularities among the various subtraction terms in eq. (6.1) takes place in just the same way as for the QCD factorization formulae described in ref. [47], with the exception of the double soft subtraction terms in eqs. (6.33) and (6.41). In this limit, the latter provide local counterterms to the squared matrix element by construction.

7. Iterated singly-unresolved counterterms

In ref. [47], we introduced the term $\mathbf{A}_{12}|\mathcal{M}^{(0)}_{m+2}|^2$ that reproduced simultaneously both the singly-unresolved limits of the doubly-unresolved limits and the doubly-unresolved limits of the singly-unresolved limits of the squared matrix element. The structure of these terms was such that $\mathbf{A}_{12}|\mathcal{M}^{(0)}_{m+2}|^2$ was defined to be $\mathbf{A}_1\mathbf{A}_2|\mathcal{M}^{(0)}_{m+2}|^2$. When extending the terms $\mathbf{A}_1|\mathcal{M}^{(0)}_{m+2}|^2$ and $\mathbf{A}_2|\mathcal{M}^{(0)}_{m+2}|^2$ over the whole phase space to obtain the subtraction terms $\boldsymbol{\mathcal{A}}_1|\mathcal{M}^{(0)}_{m+2}|^2$ and $\boldsymbol{\mathcal{A}}_2|\mathcal{M}^{(0)}_{m+2}|^2$, we defined the momentum mappings such that this structure

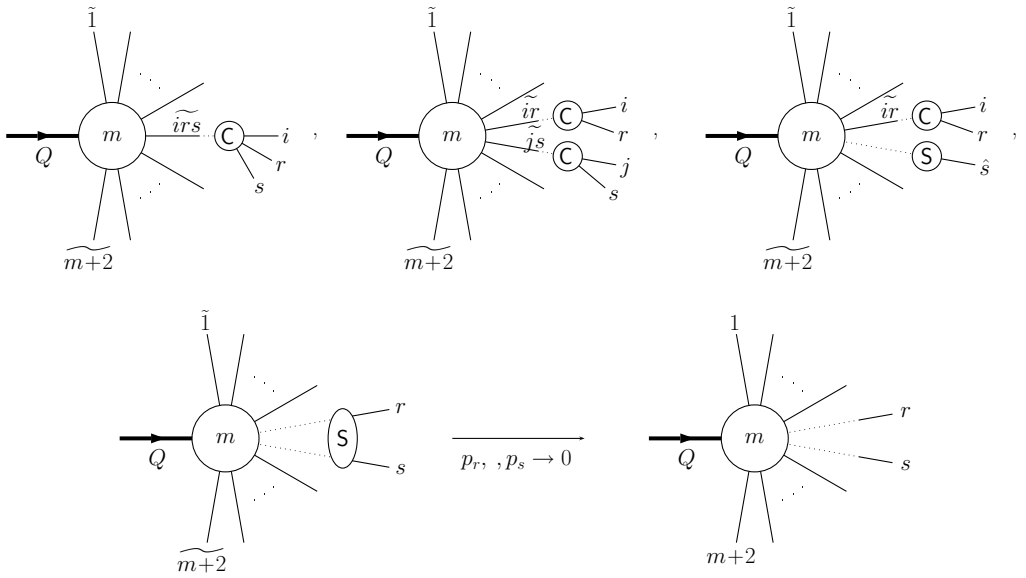

Figure 9: Graphical representation of the doubly-soft limit of the triply-, doubly-, soft-collinear and doubly-soft momentum mappings.

could be preserved, i.e., the iterated singly-unresolved counterterm $\boldsymbol{\mathcal{A}}_{12}|\mathcal{M}^{(0)}_{m+2}|^2$ is just the singly-unresolved subtraction for the doubly-unresolved counterterm $\boldsymbol{\mathcal{A}}_2|\mathcal{M}^{(0)}_{m+2}|^2$. Thus formally we can write

$$\boldsymbol{\mathcal{A}}_{12}|\mathcal{M}^{(0)}_{m+2}(\{p\})|^2 = \sum_t \Bigg[\sum_{k\neq t} \frac{1}{2}\mathcal{C}_{kt}\boldsymbol{\mathcal{A}}_2|\mathcal{M}^{(0)}_{m+2}(\{p\})|^2 + \left(\mathcal{S}_t\boldsymbol{\mathcal{A}}_2|\mathcal{M}^{(0)}_{m+2}(\{p\})|^2 - \sum_{k\neq t}\mathcal{C}_{kt}\mathcal{S}_t\boldsymbol{\mathcal{A}}_2|\mathcal{M}^{(0)}_{m+2}(\{p\})|^2 \right) \Bigg], \quad (7.1)$$

where the three terms in eq. (7.1) each evaluate further into the expressions,[7]

$$\mathcal{C}_{kt}\boldsymbol{\mathcal{A}}_2 = \sum_{r\neq k,t} \Bigg[\mathcal{C}_{kt}\mathcal{C}^{(0,0)}_{ktr} + \mathcal{C}_{kt}\mathcal{CS}^{(0,0)}_{kt;r} - \mathcal{C}_{kt}\mathcal{C}_{ktr}\mathcal{CS}^{(0,0)}_{kt;r} - \mathcal{C}_{kt}\mathcal{C}_{rkt}\mathcal{S}^{(0,0)}_{kt} + \sum_{i\neq r,k,t} \left(\frac{1}{2}\mathcal{C}_{kt}\mathcal{C}^{(0,0)}_{ir;kt} - \mathcal{C}_{kt}\mathcal{C}_{ir;kt}\mathcal{CS}^{(0,0)}_{kt;r} \right) \Bigg] + \mathcal{C}_{kt}\mathcal{S}^{(0,0)}_{kt}, \quad (7.2)$$

$$\mathcal{S}_t\boldsymbol{\mathcal{A}}_2 = \sum_{r\neq t} \Bigg\{ \sum_{i\neq r,t} \Bigg[\frac{1}{2}\left(\mathcal{S}_t\mathcal{C}^{(0,0)}_{irt} + \mathcal{S}_t\mathcal{CS}^{(0,0)}_{ir;t} - \mathcal{S}_t\mathcal{C}_{irt}\mathcal{CS}^{(0,0)}_{ir;t} \right) - \mathcal{S}_t\mathcal{C}_{irt}\mathcal{S}^{(0,0)}_{rt} - \mathcal{S}_t\mathcal{CS}_{ir;t}\mathcal{S}^{(0,0)}_{rt} + \mathcal{S}_t\mathcal{C}_{irt}\mathcal{CS}_{ir;t}\mathcal{S}^{(0,0)}_{rt} \Bigg] + \mathcal{S}_t\mathcal{S}^{(0,0)}_{rt} \Bigg\} \quad (7.3)$$

[7] At the level of the factorization formulae in ref. [47] we neglected subleading terms in the triply-collinear limit of the soft-collinear formula (see eqs. (4.33) and (4.34) in [47]), which we do not apply here. Therefore, the soft limit of the doubly-real subtraction is slightly different from that in ref. [47].

JHEP01(2007)070

and

$$\mathcal{C}_{kt}\mathcal{S}_t\boldsymbol{\mathcal{A}}_2 = \sum_{r\neq k,t}\left[\mathcal{C}_{kt}\mathcal{S}_t\mathcal{C}^{(0,0)}_{krt} + \sum_{i\neq r,k,t}\left(\frac{1}{2}\mathcal{C}_{kt}\mathcal{S}_t\mathcal{CS}^{(0,0)}_{ir;t} - \mathcal{C}_{kt}\mathcal{S}_t\mathcal{CS}_{ir;t}\mathcal{S}^{(0,0)}_{rt}\right)\right.$$
$$\left. -\mathcal{C}_{kt}\mathcal{S}_t\mathcal{C}_{krt}\mathcal{S}^{(0,0)}_{rt} - \mathcal{C}_{kt}\mathcal{S}_t\mathcal{C}_{rkt}\mathcal{S}^{(0,0)}_{kt} + \mathcal{C}_{kt}\mathcal{S}_t\mathcal{S}^{(0,0)}_{rt}\right] + \mathcal{C}_{kt}\mathcal{S}_t\mathcal{S}^{(0,0)}_{kt}. \quad (7.4)$$

In this section we spell out explicitly all subtraction terms that appear in eqs. (7.2)–(7.4). These subtraction terms are defined on factorized phase spaces that are obtained using two singly-unresolved collinear and/or soft-type mappings iteratively.

7.1 Iterated collinear counterterms

7.1.1 Iterated collinear-triple collinear counterterm

Counterterm. The counterterm corresponding to the collinear limit of the triple collinear subtraction is

$$\mathcal{C}_{kt}\mathcal{C}^{(0,0)}_{ktr}(\{p\}) = (8\pi\alpha_{\rm s}\mu^{2\varepsilon})^2\frac{1}{s_{kt}}\frac{1}{s_{\widehat{kt}\,\hat{r}}} \quad (7.5)$$
$$\times\langle\mathcal{M}^{(0)}_m(\{\tilde{p}\}^{(\widehat{kt}\,\hat{r},kt)}_m)|\hat{P}^{\text{s.o.}\,(0)}_{f_kf_tf_r}(\{z_{j,l},z_{\hat{j},\hat{l}},k_{\perp,j,l},k_{\perp,\hat{j},\hat{l}},s_{jl};\varepsilon\})|\mathcal{M}^{(0)}_m(\{\tilde{p}\}^{(\widehat{kt}\,\hat{r},kt)}_m)\rangle\,,$$

where $j,\,l = k,\,t$ and $\hat{j},\,\hat{l} = \widehat{kt}\,,\,\hat{r}$, defined in eqs. (7.12)–(7.14). Note that in our convention the ordering of the labels on the splitting kernels is usually meaningless, but in the strongly ordered kernels $\hat{P}^{\text{s.o.}\,(0)}_{f_kf_tf_r}$ the ordering matters. As a result, the same triple-parton splitting function may have different strongly-ordered limits, which can be distinguished by the momentum labels in the kernel, once the ordering of the limits is fixed by the momentum mapping, given in eq. (7.12). Thus, in the following kernels, we do not further mark the abelian and non-abelian limits as we did at the level of the factorization formulae in ref. [47]. For quark splitting we have

$$\langle s|\hat{P}^{\text{s.o.}\,(0)}_{q_r\bar{q}'_kq'_t}(z_{k,t},z_{t,k},k_{\perp,k,t},z_{\widehat{kt},\hat{r}},z_{\hat{r},\widehat{kt}},k_{\perp,\widehat{kt},\hat{r}};\varepsilon)|s'\rangle =$$
$$= T_{\rm R}\left[P^{(0)}_{q_{\hat{r}}g_{\widehat{kt}}}(z_{\hat{r},\widehat{kt}},z_{\widehat{kt},\hat{r}};\varepsilon) - 2C_{\rm F}z_{k,t}z_{t,k}\left(z_{\widehat{kt},\hat{r}} - \frac{s^2_{\hat{r}k_{\perp,k,t}}}{k^2_{\perp,k,t}s_{\widehat{kt}\,\hat{r}}}\right)\right]\delta_{ss'}\,, \quad (7.6)$$

$$\langle s|\hat{P}^{\text{s.o.}\,(0)}_{q_kg_tg_r}(z_{k,t},z_{t,k},z_{\widehat{kt},\hat{r}},z_{\hat{r},\widehat{kt}};\varepsilon)|s'\rangle = P^{(0)}_{q_kg_t}(z_{k,t},z_{t,k};\varepsilon)P^{(0)}_{q_{\widehat{kt}}g_{\hat{r}}}(z_{\widehat{kt},\hat{r}},z_{\hat{r},\widehat{kt}};\varepsilon)\delta_{ss'}\,, \quad (7.7)$$

$$\langle s|P^{\text{s.o.}\,(0)}_{q_rg_kg_t}(z_{k,t},z_{t,k},k_{\perp,k,t},z_{\widehat{kt},\hat{r}},z_{\hat{r},\widehat{kt}},k_{\perp,\widehat{kt},\hat{r}};\varepsilon)|s'\rangle = 2C_{\rm A}\left[P^{(0)}_{q_{\hat{r}}g_{\widehat{kt}}}(z_{\hat{r},\widehat{kt}},z_{\widehat{kt},\hat{r}};\varepsilon)\right.$$
$$\left.\times\left(\frac{z_{k,t}}{z_{t,k}}+\frac{z_{t,k}}{z_{k,t}}\right) + C_{\rm F}(1-\varepsilon)z_{k,t}z_{t,k}\left(z_{\widehat{kt},\hat{r}} - \frac{s^2_{\hat{r}k_{\perp,k,t}}}{k^2_{\perp,k,t}s_{\widehat{kt}\,\hat{r}}}\right)\right]\delta_{ss'}\,, \quad (7.8)$$

where $s_{\hat{r}k_{\perp,k,t}} = 2\hat{p}_r \cdot k_{\perp,k,t}$. For gluon splitting we define

$$\langle\mu|\hat{P}^{\text{s.o.}\,(0)}_{g_k q_t \bar{q}_r}(z_{k,t}, z_{t,k}, z_{\widehat{kt},\hat{r}}, z_{\hat{r},\widehat{kt}}, k_{\perp,\widehat{kt},\hat{r}}; \varepsilon)|\nu\rangle =$$

$$= P^{(0)}_{q_t g_k}(z_{t,k}, z_{k,t}; \varepsilon)\langle\mu|\hat{P}^{(0)}_{\bar{q}_{\hat{r}} q_{\widehat{tk}}}(z_{\hat{r},\widehat{tk}}, z_{\widehat{tk},\hat{r}}, k_{\perp,\hat{r},\widehat{tk}}; \varepsilon)|\nu\rangle\,, \tag{7.9}$$

$$\langle\mu|\hat{P}^{\text{s.o.}\,(0)}_{g_r q_k \bar{q}_t}(z_{k,t}, z_{t,k}, k_{\perp,k,t}, z_{\widehat{kt},\hat{r}}, z_{\hat{r},\widehat{kt}}, k_{\perp,\widehat{kt},\hat{r}}; \varepsilon)|\nu\rangle =$$

$$= 2C_{\text{A}}T_{\text{R}}\Bigg[- g^{\mu\nu}\left(\frac{z_{\hat{r},\widehat{kt}}}{z_{\widehat{kt},\hat{r}}} + \frac{z_{\widehat{kt},\hat{r}}}{z_{\hat{r},\widehat{kt}}} + z_{k,t}z_{t,k}\frac{s^2_{\hat{r}k_{\perp,k,t}}}{k^2_{\perp,k,t}s_{\widehat{kt}\,\hat{r}}}\right) + 4z_{k,t}z_{t,k}\frac{z_{\widehat{kt},\hat{r}}}{z_{\hat{r},\widehat{kt}}}\frac{k^\mu_{\perp,k,t}k^\nu_{\perp,k,t}}{k^2_{\perp,k,t}}\Bigg]$$

$$- 4C_{\text{A}}(1-\varepsilon)z_{\hat{r},\widehat{kt}}z_{\widehat{kt},\hat{r}}P^{(0)}_{q_k\bar{q}_t}(z_{k,t}, z_{t,k}, k_{\perp,k,t}; \varepsilon)\frac{k^\mu_{\perp,\hat{r},\widehat{kt}}k^\nu_{\perp,\hat{r},\widehat{kt}}}{k^2_{\perp,\hat{r},\widehat{kt}}} \tag{7.10}$$

and

$$\langle\mu|\hat{P}^{\text{s.o.}\,(0)}_{g_k g_t g_r}(z_{k,t}, z_{t,k}, k_{\perp,k,t}, z_{\widehat{kt},\hat{r}}, z_{\hat{r},\widehat{kt}}, k_{\perp,\widehat{kt},\hat{r}}; \varepsilon)|\nu\rangle = 4C^2_{\text{A}}\Bigg[- g^{\mu\nu}\left(\frac{z_{\hat{r},\widehat{kt}}}{z_{\widehat{kt},\hat{r}}} + \frac{z_{\widehat{kt},\hat{r}}}{z_{\hat{r},\widehat{kt}}}\right)$$

$$\times\left(\frac{z_{k,t}}{z_{t,k}} + \frac{z_{t,k}}{z_{k,t}}\right) + g^{\mu\nu}z_{k,t}z_{t,k}\frac{1-\varepsilon}{2}\frac{s^2_{\hat{r}k_{\perp,k,t}}}{k^2_{\perp,k,t}s_{\widehat{kt}\,\hat{r}}} - 2(1-\varepsilon)z_{k,t}z_{t,k}\frac{z_{\widehat{kt},\hat{r}}}{z_{\hat{r},\widehat{kt}}}\frac{k^\mu_{\perp,k,t}k^\nu_{\perp,k,t}}{k^2_{\perp,k,t}}\Bigg]$$

$$- 4C_{\text{A}}(1-\varepsilon)z_{\hat{r},\widehat{kt}}z_{\widehat{kt},\hat{r}}P^{(0)}_{g_k g_t}(z_{k,t}, z_{t,k}, k_{\perp,k,t}; \varepsilon)\frac{k^\mu_{\perp,\hat{r},\widehat{kt}}k^\nu_{\perp,\hat{r},\widehat{kt}}}{k^2_{\perp,\hat{r},\widehat{kt}}}\,. \tag{7.11}$$

The momentum fractions $z_{j,l}$ and the transverse momenta $k_{\perp,j,l}$ are defined in eqs. (5.7) and (5.8), respectively, with ζ_{ir} in eq. (5.10). The hatted momenta that also appear in the definition $z_{\hat{j},\hat{l}}$ and $k_{\perp,\hat{j},\hat{l}}$ are defined in eq. (7.13).

Momentum mapping and phase space factorization. The m momenta $\{\tilde{p}\}^{(\widehat{kt}\,\hat{r},kt)}_m \equiv \{\tilde{p}_1, \ldots, \tilde{p}_{\widehat{kt}\,\hat{r}}, \ldots, \tilde{p}_{m+2}\}$ appearing in the matrix elements on the right hand side of eq. (7.5) are defined in two successive collinear mappings through an intermediate set of $m+1$ momenta $\{\hat{p}\}^{(kt)}_{m+1} \equiv \{\hat{p}_1, \ldots, \hat{p}_{kt}, \ldots, \hat{p}_{m+2}\}$,

$$\{p\} \xrightarrow{\mathsf{C}_{kt}} \{\hat{p}\}^{(kt)}_{m+1} \xrightarrow{\mathsf{C}_{\widehat{kt}\,\hat{r}}} \{\tilde{p}\}^{(\widehat{kt}\,\hat{r},kt)}_m\,, \tag{7.12}$$

or explicitly

$$\hat{p}^\mu_{kt} = \frac{1}{1-\alpha_{kt}}(p^\mu_k + p^\mu_t - \alpha_{kt}Q^\mu)\,, \qquad \hat{p}^\mu_n = \frac{1}{1-\alpha_{kt}}p^\mu_n\,, \qquad n \neq k,t \tag{7.13}$$

and

$$\tilde{p}^\mu_{\widehat{kt}\,\hat{r}} = \frac{1}{1-\alpha_{\widehat{kt}\,\hat{r}}}(\hat{p}^\mu_{kt} + \hat{p}^\mu_r - \alpha_{\widehat{kt}\,\hat{r}}Q^\mu)\,, \qquad \tilde{p}^\mu_n = \frac{1}{1-\alpha_{\widehat{kt}\,\hat{r}}}\hat{p}^\mu_n\,, \qquad n \neq \widehat{kt}\,,\hat{r}\,, \tag{7.14}$$

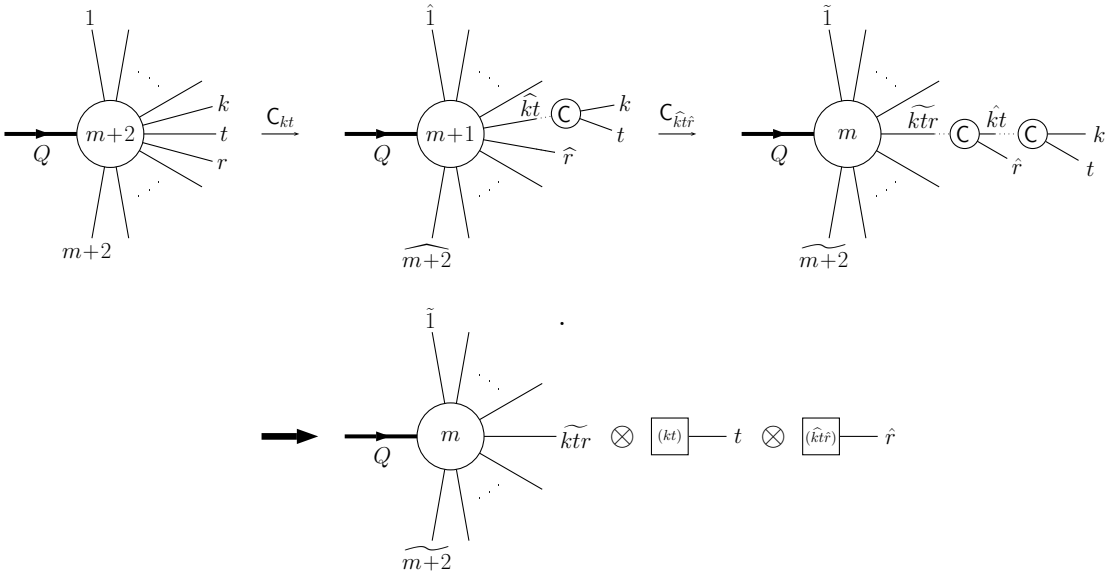

Figure 10: Graphical representation of the iterated collinear momentum mapping and the implied factorization of the phase space.

where α_{kt} and $\alpha_{\widehat{kt}\,\hat{r}}$ are given by eq. (5.12), the latter being defined on the hatted momenta.

This iterated momentum mapping leads to exact phase space factorization in the iterated form

$$\mathrm{d}\phi_{m+2}(\{p\};Q) = \mathrm{d}\phi_m(\{\tilde{p}\}_m^{(\widehat{kt}\,\hat{r},kt)};Q)[\mathrm{d}p_{1;m}^{(\widehat{kt}\,\hat{r})}(\hat{p}_r,\tilde{p}_{\widehat{kt}\,\hat{r}};Q)][\mathrm{d}p_{1;m+1}^{(kt)}(p_k,\hat{p}_{kt};Q)]\,. \tag{7.15}$$

The one-parton factorized phase spaces $[\mathrm{d}p_{1;m+1}^{(kt)}(p_k,\hat{p}_{kt};Q)]$ and $[\mathrm{d}p_{1;m}^{(\widehat{kt}\,\hat{r})}(\hat{p}_r,\tilde{p}_{\widehat{kt}\,\hat{r}};Q)]$ are given explicitly by eq. (5.16). The graphical representation of this iterated momentum mapping and the corresponding factorization of the phase space is shown in figure 10.

7.1.2 Iterated collinear-double collinear counterterm

Counterterm. Corresponding to the collinear limit of the double collinear subtraction is the counterterm

$$\begin{aligned}\mathcal{C}_{kt}\mathcal{C}_{ir;kt}^{(0,0)}(\{p\}) = (8\pi\alpha_{\mathrm{s}}\mu^{2\varepsilon})^2\frac{1}{s_{kt}}\frac{1}{s_{\hat{i}\hat{r}}} \\ \times\langle\mathcal{M}_m^{(0)}(\{\tilde{p}\}_m^{(\hat{i}\hat{r},kt)})|\hat{P}_{f_kf_t}^{(0)}(z_{k,t},z_{t,k},k_{\perp,k,t};\varepsilon)\hat{P}_{f_{\hat{i}}f_{\hat{r}}}^{(0)}(z_{\hat{i},\hat{r}},z_{\hat{r},\hat{i}},k_{\perp,\hat{i},\hat{r}};\varepsilon)|\mathcal{M}_m^{(0)}(\{\tilde{p}\}_m^{(\hat{i}\hat{r},kt)})\rangle\,.\end{aligned} \tag{7.16}$$

The variables of the Altarelli-Parisi kernels, the momentum fractions and transverse momenta, are given by eqs. (5.7) and (5.8) while the kernels themselves are recorded in eqs. (5.3)–(5.5).

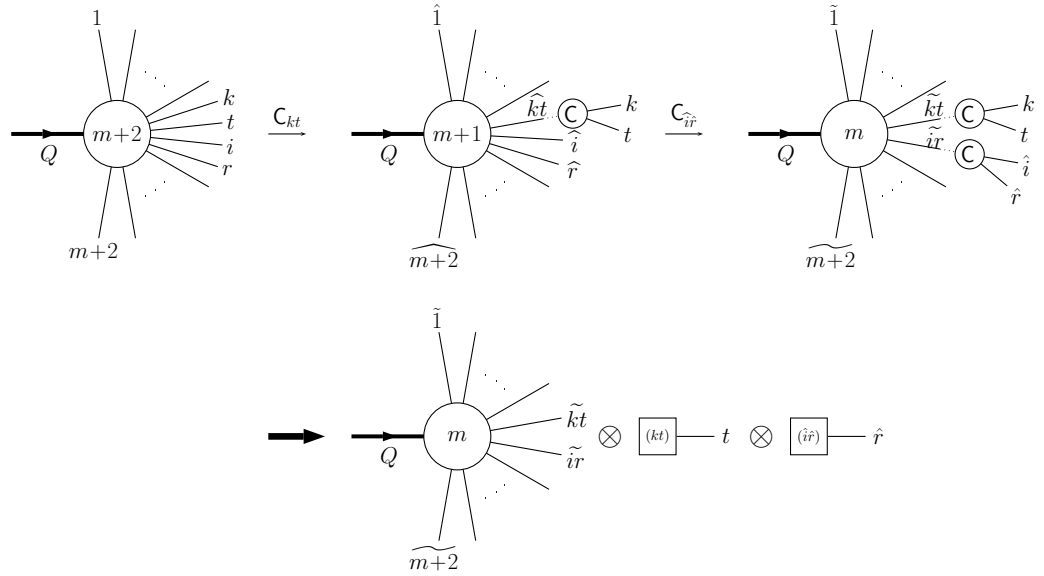

Figure 11: Graphical representation of the iterated collinear momentum mapping and the implied factorization of the phase space.

Momentum mapping and phase space factorization. The m momenta $\{\tilde{p}\}_m^{(\hat{i}\hat{r},kt)} \equiv \{\tilde{p}_1,\ldots,\tilde{p}_{\hat{i}\hat{r}},\ldots,\tilde{p}_{kt},\ldots,\tilde{p}_{m+2}\}$ in the matrix element on the right hand side of eq. (7.16) are again given by an iteration of the collinear momentum mapping of eq. (5.11),

$$\{p\} \xrightarrow{\mathsf{C}_{kt}} \{\hat{p}\}_{m+1}^{(kt)} \xrightarrow{\mathsf{C}_{\hat{i}\hat{r}}} \{\tilde{p}\}_m^{(\hat{i}\hat{r},kt)}\,. \tag{7.17}$$

The new momenta are defined as

$$\tilde{p}^\mu_{\hat{i}\hat{r}} = \frac{1}{1-\alpha_{\hat{i}\hat{r}}}(\hat{p}^\mu_i + \hat{p}^\mu_r - \alpha_{\hat{i}\hat{r}}Q^\mu)\,, \qquad \tilde{p}^\mu_n = \frac{1}{1-\alpha_{\hat{i}\hat{r}}}\hat{p}^\mu_n\,, \qquad n \neq \hat{i},\hat{r}\,, \tag{7.18}$$

where the hatted momenta that also appear in the definition $z_{\hat{i},\hat{r}}$, $z_{\hat{r},\hat{i}}$ and $k_{\perp,\hat{i},\hat{r}}$ in eq. (7.16) are defined in eq. (7.13). Again $\alpha_{\hat{i}\hat{r}}$ is given by eq. (5.12). This iterated momentum mapping leads to exact phase space factorization in the following form:

$$\mathrm{d}\phi_{m+2}(\{p\};Q) = \mathrm{d}\phi_m(\{\tilde{p}\}_m^{(\hat{i}\hat{r},kt)};Q)[\mathrm{d}p_{1;m}^{(\hat{i}\hat{r})}(\hat{p}_r,\tilde{p}_{\hat{i}\hat{r}};Q)][\mathrm{d}p_{1;m+1}^{(kt)}(p_k,\hat{p}_{kt};Q)]\,, \tag{7.19}$$

where the factorized phase space measures $[\mathrm{d}p_{1;m+1}^{(kt)}(p_k,\hat{p}_{kt};Q)]$ and $[\mathrm{d}p_{1;m}^{(\hat{i}\hat{r})}(\hat{p}_r,\tilde{p}_{\hat{i}\hat{r}};Q)]$ are given in eq. (5.16). The graphical representation of this iterated momentum mapping and the corresponding factorization of the phase space is shown in figure 11.

7.1.3 Iterated collinear–soft-collinear-type counterterms

Counterterms. The following three counterterms all use the same momentum mapping, that of the collinear–soft-collinear term $\mathcal{C}_{kt}\mathcal{CS}_{kt;r}^{(0,0)}(\{p\})$ and we present these together. We

define

$$\mathcal{C}_{kt}\mathcal{CS}^{(0,0)}_{kt;r}(\{p\}) = -(8\pi\alpha_{\rm s}\mu^{2\varepsilon})^2\sum_j\sum_{l\neq j}\frac{1}{2}\mathcal{S}_{\hat{\jmath}\hat{l}}(\hat{r}) \tag{7.20}$$
$$\times\frac{1}{s_{kt}}\langle\mathcal{M}^{(0)}_m(\{\tilde{p}\}^{(\hat{r},kt)}_m)|\boldsymbol{T}_j\boldsymbol{T}_l\hat{P}^{(0)}_{f_kf_t}(z_{k,t},z_{t,k},\tilde{k}_{\perp,k,t};\varepsilon)|\mathcal{M}^{(0)}_m(\{\tilde{p}\}^{(\hat{r},kt)}_m)\rangle\,,$$

$$\mathcal{C}_{kt}\mathcal{C}_{ir;kt}\mathcal{CS}^{(0,0)}_{kt;r}(\{p\}) = (8\pi\alpha_{\rm s}\mu^{2\varepsilon})^2\frac{2}{s_{\hat{\imath}\hat{r}}}\frac{z_{\hat{\imath},\hat{r}}}{z_{\hat{r},\hat{\imath}}}\boldsymbol{T}_i^2 \tag{7.21}$$
$$\times\frac{1}{s_{kt}}\langle\mathcal{M}^{(0)}_m(\{\tilde{p}\}^{(\hat{r},kt)}_m)|\hat{P}^{(0)}_{f_kf_t}(z_{k,t},z_{t,k},\tilde{k}_{\perp,k,t};\varepsilon)|\mathcal{M}^{(0)}_m(\{\tilde{p}\}^{(\hat{r},kt)}_m)\rangle\,,$$

$$\mathcal{C}_{kt}\mathcal{C}_{ktr}\mathcal{CS}^{(0,0)}_{kt;r}(\{p\}) = (8\pi\alpha_{\rm s}\mu^{2\varepsilon})^2\frac{2}{s_{\widehat{kt}\,\hat{r}}}\frac{z_{\widehat{kt},\hat{r}}}{z_{\hat{r},\widehat{kt}}}\boldsymbol{T}^2_{kt} \tag{7.22}$$
$$\times\frac{1}{s_{kt}}\langle\mathcal{M}^{(0)}_m(\{\tilde{p}\}^{(\hat{r},kt)}_m)|\hat{P}^{(0)}_{f_kf_t}(z_{k,t},z_{t,k},\tilde{k}_{\perp,k,t};\varepsilon)|\mathcal{M}^{(0)}_m(\{\tilde{p}\}^{(\hat{r},kt)}_m)\rangle\,.$$

As usual eq. (5.7) defines the momentum fractions and $\tilde{k}_{\perp,k,t}$ is defined in eq. (6.27).

Momentum mapping and phase space factorization. The set of m momenta $\{\tilde{p}\}^{(\hat{r},kt)}_m \equiv \{\tilde{p}_1,\ldots,\tilde{p}_{kt},\ldots,\tilde{p}_{m+2}\}$ (p_r is absent) that enter the matrix elements on the right hand sides of eqs. (7.20)–(7.22) are constructed by applying the collinear momentum mapping of eq. (5.14) followed by the soft mapping of eq. (5.26) to the original set of $m+2$ momenta $\{p\}$,

$$\{p\}\xrightarrow{\mathsf{C}_{kt}}\{\hat{p}\}^{(kt)}_{m+1}\xrightarrow{\mathsf{S}_{\hat{r}}}\{\tilde{p}\}^{(\hat{r},kt)}_m\,, \tag{7.23}$$

which we have already discussed under eq. (6.29) and shown in figure 6.

7.1.4 Iterated collinear–double-soft-type counterterms

Counterterms. The subtraction terms presented below use the same momentum mapping, thus they are discussed together. We set

$$\mathcal{C}_{kt}\mathcal{S}^{(0,0)}_{kt}(\{p\}) = (8\pi\alpha_{\rm s}\mu^{2\varepsilon})^2\sum_j\sum_l\frac{1}{2}\mathcal{S}^{\mu\nu}_{\hat{\jmath}\hat{l}}(\widehat{kt}\,)$$
$$\times\frac{1}{s_{kt}}\langle\mu|\hat{P}^{(0)}_{f_kf_t}(z_{k,t},z_{t,k},k_{\perp,k,t};\varepsilon)|\nu\rangle|\mathcal{M}^{(0)}_{m;(j,l)}(\{\tilde{p}\}^{(\widehat{kt},kt)}_m)|^2\,, \tag{7.24}$$

$$\mathcal{C}_{k_gt_g}\mathcal{C}_{rk_gt_g}\mathcal{S}^{(0,0)}_{k_gt_g}(\{p\}) = (8\pi\alpha_{\rm s}\mu^{2\varepsilon})^2\frac{2}{s_{kt}s_{\widehat{kt}\,\hat{r}}}\boldsymbol{T}_r^2C_{\rm A}$$
$$\times\left[\frac{2z_{\hat{r},\widehat{kt}}}{z_{\widehat{kt},\hat{r}}}\left(\frac{z_{k,t}}{z_{t,k}}+\frac{z_{t,k}}{z_{k,t}}\right)-(1-\varepsilon)z_{k,t}z_{t,k}\frac{s^2_{\hat{r}k_{\perp,k,t}}}{k^2_{\perp,k,t}s_{\widehat{kt}\,\hat{r}}}\right]$$
$$\times|\mathcal{M}^{(0)}_m(\{\tilde{p}\}^{(\widehat{kt},kt)}_m)|^2\,, \tag{7.25}$$

$$\mathcal{C}_{k_{\bar{q}}t_q}\mathcal{C}_{rk_{\bar{q}}t_q}\mathcal{S}^{(0,0)}_{k_{\bar{q}}t_q}(\{p\}) = (8\pi\alpha_{\rm s}\mu^{2\varepsilon})^2\frac{2}{s_{kt}s_{\widehat{kt}\,\hat{r}}}\boldsymbol{T}_r^2T_{\rm R}$$
$$\times\left(\frac{z_{\hat{r},\widehat{kt}}}{z_{\widehat{kt},\hat{r}}}+z_{k,t}z_{t,k}\frac{s^2_{\hat{r}k_{\perp,k,t}}}{k^2_{\perp,k,t}s_{\widehat{kt}\,\hat{r}}}\right)|\mathcal{M}^{(0)}_m(\{\tilde{p}\}^{(\widehat{kt},kt)}_m)|^2\,. \tag{7.26}$$

The momentum fractions and transverse momentum in eqs. (7.24)–(7.26) are defined as usual by eqs. (5.7) and (5.8). In eq. (7.24) we use the notation

$$\mathcal{S}^{\mu\nu}_{\hat{j}\hat{l}}(\widehat{kt}) = 4\frac{\hat{p}^{\mu}_{j}\hat{p}^{\nu}_{l}}{s_{\widehat{kt}\,\hat{j}}s_{\widehat{kt}\,\hat{l}}}\,. \tag{7.27}$$

The hatted momenta are given by eq. (7.13).

Momentum mapping and phase space factorization. The m momenta $\{\tilde{p}\}_m^{(\widehat{kt},kt)} \equiv \{\tilde{p}_1,\dots,\tilde{p}_{m+2}\}$ (momenta p_k and p_t are absent) that appear in the matrix elements on the right hand sides of eqs. (7.24)–(7.26) are obtained by applying the soft momentum mapping of eq. (5.26) to the hatted set of momenta of eq. (7.13),

$$\{p\} \xrightarrow{\mathsf{C}_{kt}} \{\hat{p}\}_{m+1}^{(kt)} \xrightarrow{\mathsf{S}_{\widehat{kt}}} \{\tilde{p}\}_m^{(\widehat{kt},kt)}\,. \tag{7.28}$$

We have

$$\tilde{p}^{\mu}_{n} = \Lambda^{\mu}_{\nu}[Q,(Q-p_{\widehat{kt}})/\lambda_{\widehat{kt}}](\hat{p}^{\nu}_{n}/\lambda_{\widehat{kt}})\,. \tag{7.29}$$

The hatted momenta are also used to define the momentum fractions $z_{\hat{j},\hat{l}}$ in eqs. (7.24)–(7.26) and are given in eq. (7.13).

The phase space factorization inherits the 'product' structure of the momentum mapping and we get

$$\mathrm{d}\phi_{m+2}(\{p\};Q) = \mathrm{d}\phi_m(\{\tilde{p}\}_m^{(\widehat{kt},kt)};Q)[\mathrm{d}p_{1;m}^{(\widehat{kt})}(\hat{p}_{kt};Q)][\mathrm{d}p_{1;m+1}^{(kt)}(p_k,\hat{p}_{kt};Q)]\,. \tag{7.30}$$

The one-parton factorized phase space measures $[\mathrm{d}p_{1;m+1}^{(kt)}(p_k,\hat{p}_{kt};Q)]$ and $[\mathrm{d}p_{1;m}^{(\widehat{kt})}(\hat{p}_{kt};Q)]$ are those in eqs. (5.16) and (5.28). The graphical representation of this iterated momentum mapping and the corresponding factorization of the phase space is shown in figure 12.

7.2 Iterated soft counterterms

7.2.1 Iterated soft–triple-collinear-type counterterms

Counterterms. The first three subtraction terms on the right hand side of eq. (7.3) are defined using the same momentum mapping, therefore these terms are presented together. They read

$$\begin{aligned}
\mathcal{S}_t\mathcal{C}^{(0,0)}_{irt}(\{p\}) =& (8\pi\alpha_{\mathrm{s}}\mu^{2\varepsilon})^2 P^{(\mathrm{S})}_{f_if_rf_t}(z_{i,rt},z_{r,it},z_{t,ir},s_{ir},s_{it},s_{rt};\varepsilon)\\
&\times\frac{1}{s_{\hat{i}\hat{r}}}\langle\mathcal{M}^{(0)}_m(\{\tilde{p}\}_m^{(\hat{i}\hat{r},t)})|\hat{P}^{(0)}_{f_if_r}(z_{\hat{i},\hat{r}},z_{\hat{r},\hat{i}},k_{\perp,\hat{i},\hat{r}};\varepsilon)|\mathcal{M}^{(0)}_m(\{\tilde{p}\}_m^{(\hat{i}\hat{r},t)})\rangle, \qquad (7.31)\\
\mathcal{S}_t\mathcal{C}\mathcal{S}^{(0,0)}_{ir;t}(\{p\}) =& -(8\pi\alpha_{\mathrm{s}}\mu^{2\varepsilon})^2\sum_j\sum_{l\neq j}\frac{1}{2}\mathcal{S}_{jl}(t)\\
&\times\frac{1}{s_{\hat{i}\hat{r}}}\langle\mathcal{M}^{(0)}_m(\{\tilde{p}\}_m^{(\hat{i}\hat{r},t)})|\boldsymbol{T}_j\boldsymbol{T}_l\hat{P}^{(0)}_{f_if_r}(z_{\hat{i},\hat{r}},z_{\hat{r},\hat{i}},k_{\perp,\hat{i},\hat{r}};\varepsilon)|\mathcal{M}^{(0)}_m(\{\tilde{p}\}_m^{(\hat{i}\hat{r},t)})\rangle, \qquad (7.32)\\
\mathcal{S}_t\mathcal{C}_{irt}\mathcal{C}\mathcal{S}^{(0,0)}_{ir;t}(\{p\}) =& (8\pi\alpha_{\mathrm{s}}\mu^{2\varepsilon})^2\frac{2}{s_{(ir)t}}\frac{1-z_{t,ir}}{z_{t,ir}}\boldsymbol{T}^2_{ir}\\
&\times\frac{1}{s_{\hat{i}\hat{r}}}\langle\mathcal{M}^{(0)}_m(\{\tilde{p}\}_m^{(\hat{i}\hat{r},t)})|\hat{P}^{(0)}_{f_if_r}(z_{\hat{i},\hat{r}},z_{\hat{r},\hat{i}},k_{\perp,\hat{i},\hat{r}};\varepsilon)|\mathcal{M}^{(0)}_m(\{\tilde{p}\}_m^{(\hat{i}\hat{r},t)})\rangle. \qquad (7.33)
\end{aligned}$$

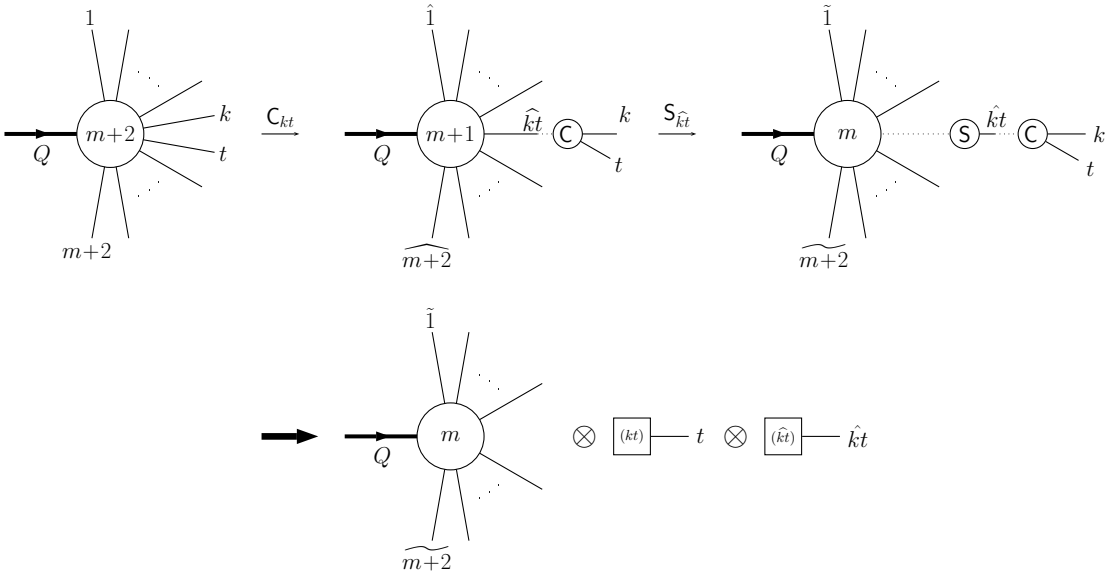

Figure 12: Graphical representation of the collinear momentum mapping followed by a soft one and the implied factorization of the phase space.

The momentum fractions $z_{j,l}$ and $z_{j,kl}$ are given respectively by eqs. (5.7) and (6.5) while the transverse momentum $k_{\perp,\hat{i},\hat{r}}$ is defined in eq. (5.8). The soft functions $P^{(\mathrm{S})}_{f_i f_r f_s}$ appearing in eq. (7.31) were introduced in ref. [47]. As discussed below eq. (6.25), whenever j or l equals (ir) the eikonal factor appearing in eq. (7.32) evaluates to the expression given in eq. (6.26).

Momentum mapping and phase space factorization. The m momenta $\{\tilde{p}\}_m^{(\hat{i}\hat{r},t)} \equiv \{\tilde{p}_1,\dots,\tilde{p}_{ir},\dots,\tilde{p}_{m+2}\}$ (p_t is absent) entering the matrix elements on the right hand sides of eqs. (7.31)–(7.33) are defined by the successive soft and collinear mappings,

$$\{p\} \xrightarrow{\mathsf{S}_t} \{\hat{p}\}_{m+1}^{(t)} \xrightarrow{\mathsf{C}_{\hat{i}\hat{r}}} \{\tilde{p}\}_m^{(\hat{i}\hat{r},t)}\,, \tag{7.34}$$

where

$$\tilde{p}^\mu_{ir} = \frac{1}{1-\alpha_{\hat{i}\hat{r}}}(\hat{p}^\mu_i + \hat{p}^\mu_r - \alpha_{\hat{i}\hat{r}}Q^\mu)\,, \qquad \tilde{p}^\mu_n = \frac{1}{1-\alpha_{\hat{i}\hat{r}}}\hat{p}^\mu_n\,, \qquad n\neq i,r \tag{7.35}$$

and the hatted momenta, that also appear in the definitions of $z_{\hat{i},\hat{r}}$, $z_{\hat{i},\hat{r}}$ and $k_{\perp,\hat{i},\hat{r}}$ in eqs. (7.31)–(7.33), are

$$\hat{p}^\mu_n = \Lambda^\mu_\nu[Q,(Q-p_t)/\lambda_t](p^\nu_n/\lambda_t)\,, \qquad n\neq t\,. \tag{7.36}$$

The expressions for $\alpha_{\hat{i}\hat{r}}$ in eq. (7.35) and λ_t in eq. (7.36) are given in eqs. (5.12) and (5.23) respectively. This momentum mapping leads to an exact phase space factorization of the following form

$$\mathrm{d}\phi_{m+2}(\{p\};Q) = \mathrm{d}\phi_m(\{\tilde{p}\}_m^{(\hat{i}\hat{r},t)};Q)[\mathrm{d}p^{(\hat{i}\hat{r})}_{1;m}(\hat{p}_r,\tilde{p}_{ir};Q)][\mathrm{d}p^{(t)}_{1;m+1}(p_t;Q)]\,. \tag{7.37}$$

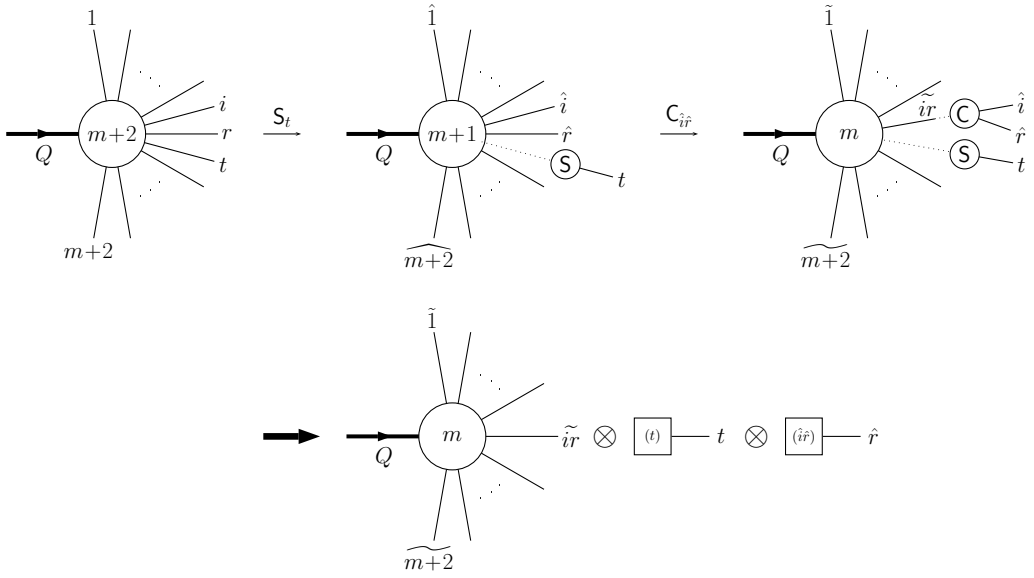

Figure 13: Graphical representation of the soft momentum mapping followed by a collinear one and the implied factorization of the phase space.

The collinear and soft one-parton factorized phase space measures $[\mathrm{d}p^{(\hat{i}\hat{r})}_{1;m}(\hat{p}_r, \tilde{p}_{ir}; Q)]$ and $[\mathrm{d}p^{(t)}_{1;m+1}(p_t; Q)]$ are given respectively in eqs. (5.16) and (5.28). The graphical representation of this iterated momentum mapping and the corresponding factorization of the phase space is shown in figure 13.

7.2.2 Iterated soft–double-soft-type counterterms

Counterterms. The remaining four iterated soft counterterms in eq. (7.3) are all defined using the same momentum mapping so we discuss them together. We have

$$\mathcal{S}_t\mathcal{C}_{irt}\mathcal{S}^{(0,0)}_{rt}(\{p\}) = (8\pi\alpha_{\mathrm{s}}\mu^{2\varepsilon})^2\Bigg[C_{\mathrm{A}}\frac{2}{s_{\hat{i}\hat{r}}}\frac{z_{\hat{i},\hat{r}}}{z_{\hat{r},\hat{i}}}\left(\frac{s_{ir}}{s_{it}s_{rt}}+\frac{1}{s_{rt}}\frac{z_{r,it}}{z_{t,ir}}-\frac{1}{s_{it}}\frac{z_{i,rt}}{z_{t,ir}}\right) + \boldsymbol{T}_i^2\frac{2}{s_{it}}\frac{z_{i,t}}{z_{t,i}}\frac{2}{s_{\hat{i}\hat{r}}}\frac{z_{\hat{i},\hat{r}}}{z_{\hat{r},\hat{i}}}\Bigg]\boldsymbol{T}_i^2|\mathcal{M}^{(0)}_m(\{\tilde{p}\}^{(\hat{r},t)}_m)|^2\,, \tag{7.38}$$

$$\mathcal{S}_t\mathcal{C}\mathcal{S}_{ir;t}\mathcal{S}^{(0,0)}_{rt}(\{p\}) = -(8\pi\alpha_{\mathrm{s}}\mu^{2\varepsilon})^2\frac{2}{s_{\hat{i}\hat{r}}}\frac{z_{\hat{i},\hat{r}}}{z_{\hat{r},\hat{i}}}\boldsymbol{T}_i^2\sum_j\sum_{l\neq j}\frac{1}{2}\mathcal{S}_{jl}(t)|\mathcal{M}^{(0)}_{m;(j,l)}(\{\tilde{p}\}^{(\hat{r},t)}_m)|^2\,, \tag{7.39}$$

$$\mathcal{S}_t\mathcal{C}_{irt}\mathcal{C}\mathcal{S}_{ir;t}\mathcal{S}^{(0,0)}_{rt}(\{p\}) = (8\pi\alpha_{\mathrm{s}}\mu^{2\varepsilon})^2\,\boldsymbol{T}_i^2\,\frac{2}{s_{\hat{i}\hat{r}}}\frac{z_{\hat{i},\hat{r}}}{z_{\hat{r},\hat{i}}}\frac{2}{s_{(ir)t}}\frac{1-z_{t,ir}}{z_{t,ir}}\boldsymbol{T}_i^2\,|\mathcal{M}^{(0)}_m(\{\tilde{p}\}^{(\hat{r},t)}_m)|^2\,, \tag{7.40}$$

$$\mathcal{S}_t\mathcal{S}^{(0,0)}_{rt}(\{p\}) = (8\pi\alpha_{\mathrm{s}}\mu^{2\varepsilon})^2\Bigg[\frac{1}{8}\sum_{i,j,k,l}\mathcal{S}_{\hat{i}\hat{k}}(\hat{r})\mathcal{S}_{jl}(t)|\mathcal{M}^{(0)}_{m;(i,k)(j,l)}(\{\tilde{p}\}^{(\hat{r},t)}_m)|^2 - \frac{1}{4}C_{\mathrm{A}}\sum_{i,k}\mathcal{S}_{\hat{i}\hat{k}}(\hat{r})\Big(\mathcal{S}_{ir}(t)+\mathcal{S}_{kr}(t)-\mathcal{S}_{ik}(t)\Big)|\mathcal{M}^{(0)}_{m;(i,k)}(\{\tilde{p}\}^{(\hat{r},t)}_m)|^2\Bigg]\,. \tag{7.41}$$

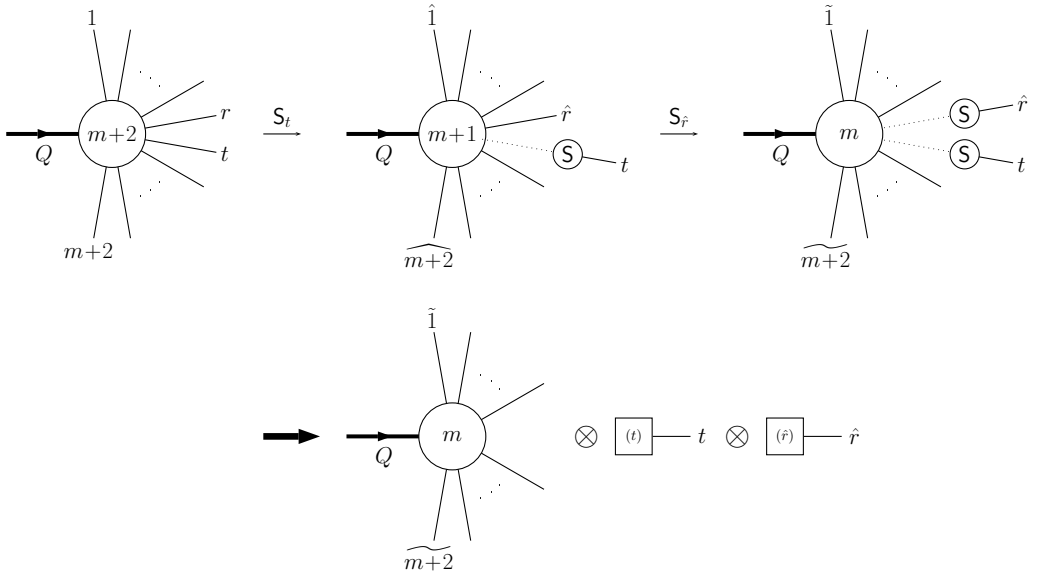

Figure 14: Graphical representation of the iterated soft momentum mapping and the implied factorization of the phase space.

No new notation (besides the set of momenta $\{\tilde{p}\}_m^{(\hat{r},t)}$ to be defined below) has been introduced in eqs. (7.38)–(7.41), thus we limit the discussion of these terms to two comments. Firstly, note that in the equations above both r and t are gluons. Secondly, we emphasize that the discussion below eq. (6.25) also applies to eq. (7.39).

Momentum mapping and phase space factorization. The m momenta $\{\tilde{p}\}_m^{(\hat{r},t)} \equiv \{\tilde{p}_1, \ldots, \tilde{p}_{m+2}\}$ (both r and t are omitted) that appear in the matrix elements on the right hand sides of eqs. (7.38)–(7.41) are obtained by two successive soft-type mappings (defined in eq. (5.22)),

$$\{p\} \xrightarrow{\mathsf{S}_t} \{\hat{p}\}_{m+1}^{(t)} \xrightarrow{\mathsf{S}_{\hat{r}}} \{\tilde{p}\}_m^{(\hat{r},t)}\,, \tag{7.42}$$

where

$$\tilde{p}_n^\mu = \Lambda_\nu^\mu[Q, (Q-\hat{p}_r)/\lambda_{\hat{r}}](\hat{p}_n^\nu/\lambda_{\hat{r}})\,, \qquad n \neq r\,. \tag{7.43}$$

The hatted momenta are given in eq. (7.36). Naturally, the iterative structure of the momentum mapping is inherited by the phase space factorization

$$\mathrm{d}\phi_{m+2}(\{p\};Q) = \mathrm{d}\phi_m(\{\tilde{p}\}_m^{(\hat{r},t)};Q)[\mathrm{d}p_{1;m}^{(\hat{r})}(\hat{p}_r;Q)][\mathrm{d}p_{1;m+1}^{(t)}(p_t;Q)]\,, \tag{7.44}$$

where the soft one-parton factorized phase space measures $[\mathrm{d}p_{1;m}^{(\hat{r})}(\hat{p}_r;Q)]$ and $[\mathrm{d}p_{1;m+1}^{(t)}(p_t;Q)]$ are both given by eq. (5.28). The graphical representation of this iterated momentum mapping and the corresponding factorization of the phase space is shown in figure 14.

7.3 Iterated soft-collinear counterterms

7.3.1 Iterated soft-collinear–triple-collinear-type counterterms

Counterterms. The first two terms on the right hand side of eq. (7.4) turn out to be defined using the same momentum mapping after a trivial reindexing. Let us define

$$\begin{aligned}\mathcal{C}_{it}\mathcal{S}_t\mathcal{C}^{(0,0)}_{irt} &= (8\pi\alpha_{\mathrm{s}}\mu^{2\varepsilon})^2\frac{2}{s_{it}}\frac{z_{i,t}}{z_{t,i}}\boldsymbol{T}^2_{it} \\ &\quad\times\frac{1}{s_{\hat{i}\hat{r}}}\langle\mathcal{M}^{(0)}_m(\{\tilde{p}\}^{(\hat{i}\hat{r},t)}_m)|\hat{P}^{(0)}_{f_if_r}(z_{\hat{i},\hat{r}},z_{\hat{r},\hat{i}},k_{\perp,\hat{i},\hat{r}};\varepsilon)|\mathcal{M}^{(0)}_m(\{\tilde{p}\}^{(\hat{i}\hat{r},t)}_m)\rangle\,, \quad (7.45)\\ \mathcal{C}_{kt}\mathcal{S}_t\mathcal{C}\mathcal{S}^{(0,0)}_{ir;t}(\{p\}) &= (8\pi\alpha_{\mathrm{s}}\mu^{2\varepsilon})^2\frac{2}{s_{kt}}\frac{z_{k,t}}{z_{t,k}}\boldsymbol{T}^2_{i} \\ &\quad\times\frac{1}{s_{\hat{i}\hat{r}}}\langle\mathcal{M}^{(0)}_m(\{\tilde{p}\}^{(\hat{i}\hat{r},t)}_m)|\hat{P}^{(0)}_{f_if_r}(z_{\hat{i},\hat{r}},z_{\hat{r},\hat{i}},k_{\perp,\hat{i},\hat{r}};\varepsilon)|\mathcal{M}^{(0)}_m(\{\tilde{p}\}^{(\hat{i}\hat{r},t)}_m)\rangle\,. \quad (7.46)\end{aligned}$$

Notice how a different indexing of $\mathcal{C}_{it}\mathcal{S}_t\mathcal{C}^{(0,0)}_{irt}(\{p\})$ is given above as compared to that appearing in eq. (7.4). As already stated, this is convenient, because with this indexing exactly the same set of tilded momenta, $\{\tilde{p}\}^{(\hat{i}\hat{r},t)}_m$, appear in the matrix elements on the right hand sides of both eqs. (7.45) and (7.46). The momentum fractions and transverse momenta are defined as usual via eqs. (5.7) and (5.8).

Momentum mapping and phase space factorization. Exactly the same momentum mapping is used as for the iterated soft–triple-collinear-type counterterms, section 7.2.1.

7.3.2 Iterated soft-collinear–double-soft-type counterterms

Counterterms. The remaining five terms on the right hand side of eq. (7.4) are again defined using the same momentum mapping after reindexing some terms. We have

$$\mathcal{C}_{kt}\mathcal{S}_t\mathcal{C}\mathcal{S}_{ir;t}\mathcal{S}^{(0,0)}_{rt}(\{p\}) = (8\pi\alpha_{\mathrm{s}}\mu^{2\varepsilon})^2\frac{2}{s_{\hat{i}\hat{r}}}\frac{z_{\hat{i},\hat{r}}}{z_{\hat{r},\hat{i}}}\boldsymbol{T}^2_{ir}\,\frac{2}{s_{kt}}\frac{z_{k,t}}{z_{t,k}}\boldsymbol{T}^2_{k}\,|\mathcal{M}^{(0)}_m(\{\tilde{p}\}^{(\hat{r},t)}_m)|^2\,, \quad (7.47)$$

$$\mathcal{C}_{kt}\mathcal{S}_t\mathcal{C}_{krt}\mathcal{S}^{(0,0)}_{rt}(\{p\}) = (8\pi\alpha_{\mathrm{s}}\mu^{2\varepsilon})^2\frac{2}{s_{\hat{k}\hat{r}}}\frac{z_{\hat{k},\hat{r}}}{z_{\hat{r},\hat{k}}}\boldsymbol{T}^2_{kr}\,\frac{2}{s_{kt}}\frac{z_{k,t}}{z_{t,k}}\boldsymbol{T}^2_{k}\,|\mathcal{M}^{(0)}_m(\{\tilde{p}\}^{(\hat{r},t)}_m)|^2\,, \quad (7.48)$$

$$\mathcal{C}_{rt}\mathcal{S}_t\mathcal{C}_{krt}\mathcal{S}^{(0,0)}_{rt}(\{p\}) = (8\pi\alpha_{\mathrm{s}}\mu^{2\varepsilon})^2\frac{2}{s_{\hat{k}\hat{r}}}\frac{z_{\hat{k},\hat{r}}}{z_{\hat{r},\hat{k}}}\boldsymbol{T}^2_{kr}\,\frac{2}{s_{rt}}\frac{z_{r,t}}{z_{t,r}}\,C_{\mathrm{A}}\,|\mathcal{M}^{(0)}_m(\{\tilde{p}\}^{(\hat{r},t)}_m)|^2\,, \quad (7.49)$$

$$\mathcal{C}_{kt}\mathcal{S}_t\mathcal{S}^{(0,0)}_{rt}(\{p\}) = -(8\pi\alpha_{\mathrm{s}}\mu^{2\varepsilon})^2\sum_j\sum_{l\neq j}\frac{1}{2}\mathcal{S}_{\hat{j}\hat{l}}(\hat{r})\frac{2}{s_{kt}}\frac{z_{k,t}}{z_{t,k}}\boldsymbol{T}^2_{k}|\mathcal{M}^{(0)}_{m;(j,l)}(\{\tilde{p}\}^{(\hat{r},t)}_m)|^2\,, \quad (7.50)$$

$$\mathcal{C}_{rt}\mathcal{S}_t\mathcal{S}^{(0,0)}_{rt}(\{p\}) = -(8\pi\alpha_{\mathrm{s}}\mu^{2\varepsilon})^2\sum_j\sum_{l\neq j}\frac{1}{2}\mathcal{S}_{\hat{j}\hat{l}}(\hat{r})\frac{2}{s_{rt}}\frac{z_{r,t}}{z_{t,r}}C_{\mathrm{A}}|\mathcal{M}^{(0)}_{m;(j,l)}(\{\tilde{p}\}^{(\hat{r},t)}_m)|^2\,. \quad (7.51)$$

Here $\mathcal{C}_{rt}\mathcal{S}_t\mathcal{C}_{krt}\mathcal{S}^{(0,0)}_{rt}(\{p\})$ and $\mathcal{C}_{rt}\mathcal{S}_t\mathcal{S}^{(0,0)}_{rt}(\{p\})$ are presented with a different indexing then in eq. (7.4) so that all matrix elements on the right hand sides of eqs. (7.47)–(7.51) appear with the same set of tilded momenta, $\{\tilde{p}\}^{(\hat{r},t)}_m$. The momentum fractions have been defined in eq. (5.7), the eikonal factor in eq. (5.21).

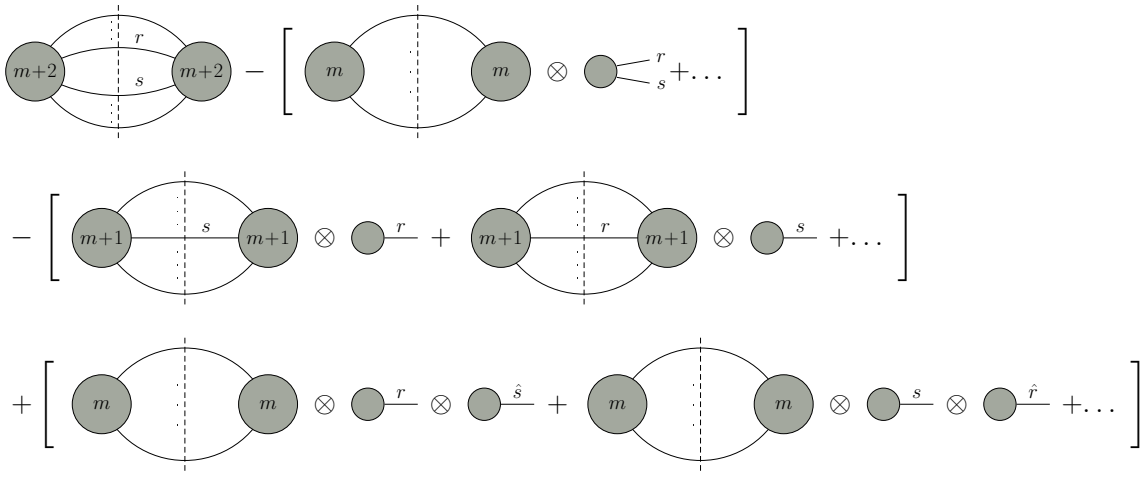

Figure 15: Graphical representation of the squared matrix element and its factorization formulae in the singly- and doubly-unresolved (soft and/or collinear) limits.

Momentum mapping and phase space factorization. The momentum mapping used is identical with the mapping defined for the iterated soft–double-soft-type counterterms. This mapping and the corresponding phase space factorization is presented in section 7.2.2.

8. Cancellation of kinematical singularities

In section 5, we have shown that the subtraction terms collected in eq. (5.1) correctly regularize the kinematical singularities in the squared matrix element in the singly-unresolved regions of the phase space. Similarly, the subtraction terms collected in eq. (6.1) correctly regularize the kinematical singularities in the doubly-unresolved regions of the phase space. The purpose of the iterated counterterms is two-fold. These should cancel the kinematical singularities of the singly-unresolved counterterms in the doubly-unresolved regions of the phase space and conversely, they should cancel the kinematical singularities of the doubly-unresolved counterterms in the singly-unresolved regions of the phase space. The structure of eq. (7.1) follows that of the candidate subtraction term $\mathbf{A}_{12}|\mathcal{M}^{(0)}_{m+2}|^2$ found in ref. [47], where it was shown that at the level of the factorization formulae the combination $(\mathbf{A}_2+\mathbf{A}_1-\mathbf{A}_{12})|\mathcal{M}^{(0)}_{m+2}|^2$ indeed regularizes the squared matrix element in all relevant unresolved regions of the phase space. We show the structure of the cancellations graphically in figure 15.

The first picture corresponds to the squared matrix element of the $m+2$ final-state partons, while the following terms in the squared brackets correspond to the terms that build $\mathbf{A}_2|\mathcal{M}^{(0)}_{m+2}|^2$, $\mathbf{A}_1|\mathcal{M}^{(0)}_{m+2}|^2$ and $\mathbf{A}_{12}|\mathcal{M}^{(0)}_{m+2}|^2$, respectively. The factorized one- and two-parton factors correspond to Altarelli-Parisi kernels, with azimuthal correlations included, or eikonal factors, with colour-correlations included, or the combinations of these. In the first bracket we find all those terms that regularize the kinematical singularities of the squared matrix element in the doubly-unresolved regions of the phase space. In these

JHEP01(2007)070

phase space regions the terms in the second bracket, corresponding to $\mathbf{A}_1|\mathcal{M}^{(0)}_{m+2}|^2$, are regularized by terms in the third bracket, corresponding to $\mathbf{A}_{12}|\mathcal{M}^{(0)}_{m+2}|^2$. In particular, if partons r and s become unresolved, than the two terms shown in the third line regularize those two in the second line.

In the singly-unresolved regions, the second bracket contains all terms, necessary to regularize the squared matrix element. Note however, that these terms also contain spurious singularities. For instance, when r is unresolved, then the first term in the second bracket regularizes the squared matrix element, while the second becomes singular. This term will be regularized by the second term in the third bracket. At the same time, the terms in the first bracket will lead to a strongly-ordered factorization formula, that will be regularized by the first term in the third bracket. If s becomes unresolved, then the role of the two terms in the third bracket interchanges: the first term will regularize the spurious singularity in the first term of the second bracket, while the second will regularize the term in the first bracket.

In defining the full subtraction $(\boldsymbol{\mathcal{A}}_2 + \boldsymbol{\mathcal{A}}_1 - \boldsymbol{\mathcal{A}}_{12})|\mathcal{M}^{(0)}_{m+2}|^2$, we keep the structure of $(\mathbf{A}_2 + \mathbf{A}_1 - \mathbf{A}_{12})|\mathcal{M}^{(0)}_{m+2}|^2$ and replace the momenta in the squared matrix elements of m or $m+1$ final-state partons in figure 15 with tilded momenta, defined by different types of momentum mappings for the various terms. In order that the cancellations described in the previous two paragraphs take place it is crucial that these momentum mappings obey the following three conditions:

1. The mappings used for defining the doubly-unresolved subtraction terms should be such that in the singly-unresolved regions of the phase space, the mapped momenta tend to the same limit as those of the iterated mappings, used for defining the terms in $\boldsymbol{\mathcal{A}}_{12}|\mathcal{M}^{(0)}_{m+2}|^2$.
2. In those regions of the phase space, where only momentum p_s^μ becomes unresolved, the singly-collinear and soft momentum mappings, used in the definition of those singly-unresolved subtraction terms, in which momentum p_r^μ is factorized, tend to the same limit as the iterated mappings used in the definition of those terms in $\boldsymbol{\mathcal{A}}_{12}|\mathcal{M}^{(0)}_{m+2}|^2$, in which the first mapping factorizes p_r^μ and the second $\hat{p}_s^\mu$.
3. In the doubly-unresolved regions of the phase space, the singly-collinear and soft momentum mappings, used in the definition of the $\boldsymbol{\mathcal{A}}_1|\mathcal{M}^{(0)}_{m+2}|^2$ term, tend to the same limit as the iterated mappings used in the definition of $\boldsymbol{\mathcal{A}}_{12}|\mathcal{M}^{(0)}_{m+2}|^2$.

The first of these conditions is necessary in order that the required cancellations between $\boldsymbol{\mathcal{A}}_2|\mathcal{M}^{(0)}_{m+2}|^2$ and $\boldsymbol{\mathcal{A}}_{12}|\mathcal{M}^{(0)}_{m+2}|^2$ take place. The second requirement ensures that the cancellations between the first terms in the second and third bracket of figure 15 happens when momentum p_s^μ becomes unresolved. Finally, the third condition is needed for cancelling all kinematical singularities of the $\boldsymbol{\mathcal{A}}_1|\mathcal{M}^{(0)}_{m+2}|^2$ terms by the corresponding terms in $\boldsymbol{\mathcal{A}}_{12}|\mathcal{M}^{(0)}_{m+2}|^2$ in the doubly-unresolved regions of the phase space. It is not difficult to check that the above requirements are fulfilled for all mappings. In particular, the third condition follows from the construction of the iterative mappings, namely these are suc-

JHEP01(2007)070

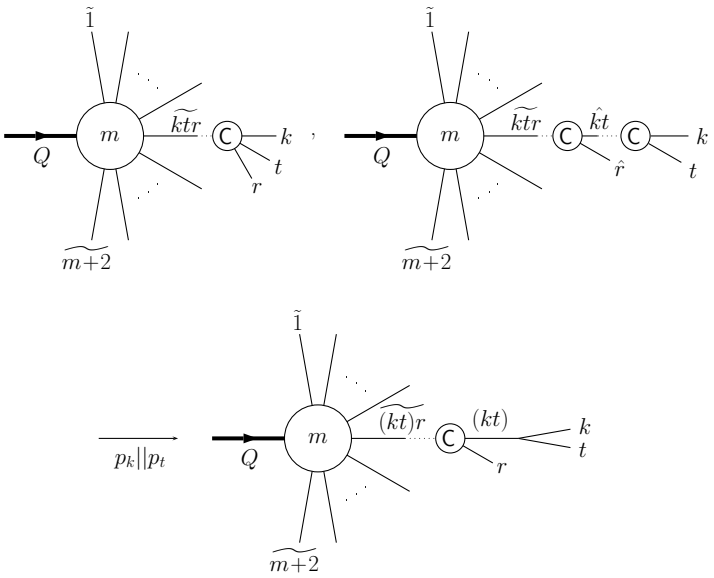

Figure 16: Graphical representation of the collinear limit of the triply-collinear and and iterated singly-collinear mappings. (kt) means the momentum $p_k^\mu + p_t^\mu$ in the collinear direction in the collinear limit.

cessive applications of the singly-collinear and/or soft mappings. Here we consider two illustrative examples of the first two conditions.

In the case of the first condition, the least trivial is that the singly-collinear limit of the triply-collinear mapping is the same as that of two successive collinear mappings, defined by eqs. (7.12)–(7.14), as shown graphically in figure 16. In the limit when momenta p_k^μ and p_t^μ are collinear, using eqs. (6.5) and (6.6) we find

$$z_{k,ts} \xrightarrow[p_k||p_t]{} z_k z_{(kt),s}\,, \qquad z_{t,ks} \xrightarrow[p_k||p_t]{} z_t z_{(kt),s}\,, \qquad z_{s,kt} \xrightarrow[p_k||p_t]{} z_{s,(kt)} \tag{8.1}$$

and

$$k^\mu_{\perp,k,ts} \xrightarrow[p_k||p_t]{} z_k k^\mu_{\perp,(kt),s}\,, \qquad k^\mu_{\perp,t,ks} \xrightarrow[p_k||p_t]{} z_t k^\mu_{\perp,(kt),s}\,, \qquad k^\mu_{\perp,s,kt} \xrightarrow[p_k||p_t]{} k^\mu_{\perp,s,(kt)}\,, \tag{8.2}$$

i.e., both the momentum fractions and the transverse momenta tend to the limit of the corresponding variables of the iterative collinear mapping. As a result, the kinematics defined by the two mappings tends to the same limit and the cancellation of the singularities takes place.

For the second requirement, let us consider for example, the soft limit $p_s^\mu \to 0$. The singly-unresolved counterterms depend on $\tilde{p}_s^\mu$, while the iterated terms depend on $\hat{p}_s^\mu$. The singly-unresolved mappings, that lead to these different momenta in the two cases, are linear in p_s^μ, therefore, $\hat{p}_s^\mu \to 0$ in the soft limit, when $p_s^\mu \to 0$. It follows that $\lambda_{\hat{s}} \to 1$ when $p_s^\mu \to 0$ so in the soft limit the hatted momenta tend to those with tilde. In particular, $\hat{p}_s^\mu \to \tilde{p}_s^\mu$ if $p_s^\mu \to 0$, so the kinematics become identical and the cancellation takes place. The graphical representations of the soft limits of the two mappings are shown in figure 17.

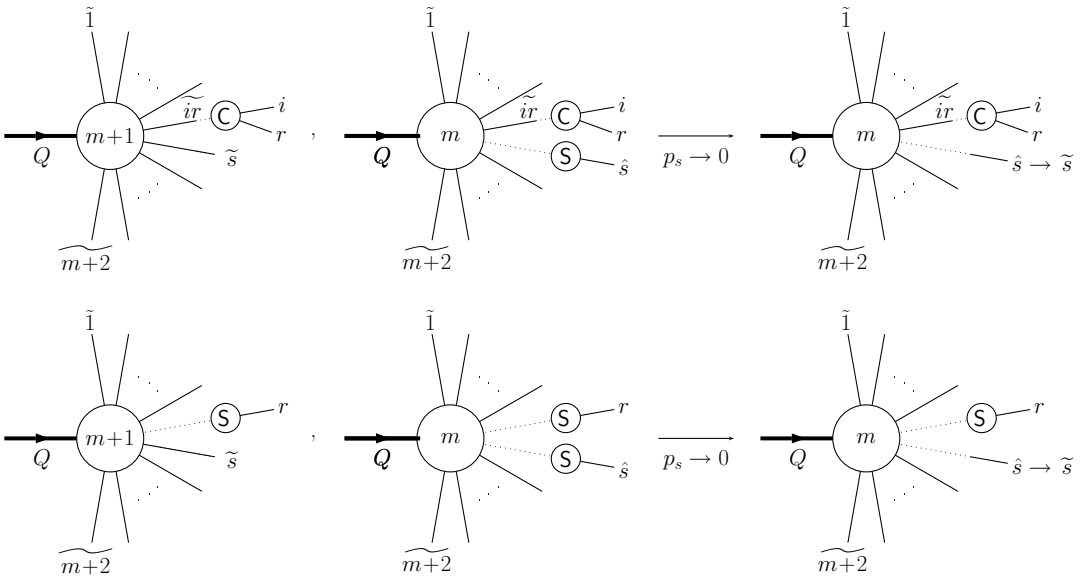

Figure 17: Graphical representation of the soft limit of the singly-unresolved and iterated momentum mappings.

9. Numerical results

In sections 5, 6 and 7 we have defined explicitly all subtraction terms in eqs. (4.3)–(4.5) that are necessary to make $\mathrm{d}\sigma^{\mathrm{RR}}_{m+2}$ integrable in $d = 4$ dimensions. In order to further demonstrate that the subtraction terms indeed regularize the cross section for doubly-real emission, we consider the non-trivial example of the contribution of the $e^+e^- \to q\bar{q}ggg$ subprocess to the moments of three-jet event-shape variables thrust (T) and C-parameter, when the jet function is a functional

$$J_n(p_1, \ldots, p_n; O) = \delta(O - O_3(p_1, \ldots, p_n)) \,, \tag{9.1}$$

with $O_3(p_1, \ldots, p_n)$ being the value of either $\tau \equiv 1 - T$ or C for a given event $(p_1, \ldots, p_n)$. The $e^+e^- \to q\bar{q}ggg$ subprocess gives rise to the most general kinds of kinematical singularities and colour structures. The only additional complication present in the four-quark subprocess $e^+e^- \to q\bar{q}Q\bar{Q}g$ is the identical flavour contribution that does not require any addition to the subtraction scheme.

Starting from randomly chosen phase space points and approaching the various singly- and doubly-unresolved regions of the phase space in successive steps, we have checked numerically that the sum of the subtraction terms has the same limits (up to integrable square-root singularities) as the squared matrix element itself.

The perturbative expansion to the n^{th} moment of a three-jet observable at a fixed scale $\mu = Q$ and NNLO accuracy can be parametrized as

$$\begin{aligned} \langle O^n \rangle &\equiv \int \mathrm{d}O \, O^n \, \frac{1}{\sigma_0} \frac{\mathrm{d}\sigma}{\mathrm{d}O} = \\ &= \left(\frac{\alpha_{\mathrm{s}}(Q)}{2\pi}\right) A_O^{(n)} + \left(\frac{\alpha_{\mathrm{s}}(Q)}{2\pi}\right)^2 B_O^{(n)} + \left(\frac{\alpha_{\mathrm{s}}(Q)}{2\pi}\right)^3 C_O^{(n)} \,, \end{aligned} \tag{9.2}$$

n	$C^{(n)}_{\tau;5}$	$C^{(n)}_{C;5}$
1	-$(9.27 \pm 0.33) \cdot 10$	-$(3.44 \pm 0.13) \cdot 10^2$
2	-$(0.31 \pm 0.04) \cdot 10$	-$(1.41 \pm 0.03) \cdot 10^2$
3	-$(0.20 \pm 0.01) \cdot 10$	-$(0.63 \pm 0.18) \cdot 10$

Table 1: The moments $C^{(n)}_{\tau;5}$ and $C^{(n)}_{C;5}$.

where according to eq. (3.4), the NNLO correction is a sum of three contributions

$$C^{(n)}_O = C^{(n)}_{O;5} + C^{(n)}_{O;4} + C^{(n)}_{O;3}\,. \tag{9.3}$$

Carrying out the phase space integrations in eq. (3.5), we computed the five-parton contribution $C^{(n)}_{O;5}(O)$ as defined in this article. The predictions for the first three moments of τ and the C-parameter, obtained using about ten million Monte Carlo events, are presented in table 1. These numbers are unphysical, and given only to demonstrate that the $(m+2)$-parton NNLO cross section defined in this paper is finite. In particular, the relatively small negative values simply indicate that the subtractions altogether subtract slightly more then the full doubly-real cross section. If needed, the colour decomposition is straightforward.

10. Conclusions

In this paper we have presented a generalization of the dipole subtraction scheme for computing NNLO corrections to QCD jet cross sections to processes without coloured partons in the initial state. The scheme is completely general in the sense that any number of massless coloured final-state partons (massive vector bosons are assumed to decay into massless fermions) are allowed provided the necessary squared matrix elements are known. It is also general in the sense that it is algorithmic in a straightforward manner, therefore, the generalization to N^{n}LO accuracy does not require new concepts. Each step of the computation can in principle be extended to any order in perturbation theory, which is useful in setting up parton shower algorithms that can be matched to fixed-order approximations naturally.

Three types of corrections contribute to the NNLO corrections: the doubly-real, the real-virtual and the doubly-virtual ones. Here we have constructed the subtraction terms for the doubly-real emissions; those to the real-virtual corrections will be presented in a companion paper. By rendering these two contributions finite in $d = 4$ dimensions, the KLN theorem ensures that for infrared safe observables adding the subtractions above to the doubly-virtual correction, that becomes also finite in $d = 4$ dimensions.

The subtraction terms for the doubly-real corrections presented here are local in $d = 4-2\varepsilon$ dimensions and include complete colour and azimuthal correlations. The expressions were derived by extending the various singly- and doubly-unresolved limits of QCD squared matrix elements over the whole phase space, which was achieved by introducing momentum mappings which define exactly factorized phase-space measures. Although the number of subtraction terms is rather large, the implementation of the scheme is not so complicated,

JHEP01(2007)070

because only five different types of phase-space mappings have to be defined, all other mappings being obtained by employing those five basic ones iteratively.

In order to demonstrate that the subtracted cross section is indeed integrable, we have computed the corresponding contributions to the first three moments of two three-jet event-shape observables, the thrust and the C-parameter.

Acknowledgments

We are grateful to Z. Nagy for his comments on choosing the transverse momenta and for the hospitality of the CERN Theory Division, where this work was completed. This research was supported in part by the Hungarian Scientific Research Fund grant OTKA K-60432.

References

[1] W.T. Giele and E.W.N. Glover, *Higher order corrections to jet cross-sections in e^+e^- annihilation*, *Phys. Rev.* **D 46** (1992) 1980.

[2] W.T. Giele, E.W.N. Glover and D.A. Kosower, *Higher order corrections to jet cross-sections in hadron colliders*, *Nucl. Phys.* **B 403** (1993) 633 [hep-ph/9302225].

[3] S. Frixione, Z. Kunszt and A. Signer, *Three-jet cross sections to next-to-leading order*, *Nucl. Phys.* **B 467** (1996) 399 [hep-ph/9512328].

[4] Z. Nagy and Z. Trócsányi, *Calculation of QCD jet cross sections at next-to-leading order*, *Nucl. Phys.* **B 486** (1997) 189 [hep-ph/9610498].

[5] S. Frixione, *A general approach to jet cross sections in QCD*, *Nucl. Phys.* **B 507** (1997) 295 [hep-ph/9706545].

[6] S. Catani and M.H. Seymour, *A general algorithm for calculating jet cross sections in NLO QCD*, *Nucl. Phys.* **B 485** (1997) 291 *Erratum ibid.* **B 510** (1997) 291[hep-ph/9605323].

[7] S. Moch, J.A.M. Vermaseren and A. Vogt, *The three-loop splitting functions in QCD: the non-singlet case*, *Nucl. Phys.* **B 688** (2004) 101 [hep-ph/0403192];
A. Vogt, S. Moch and J.A.M. Vermaseren, *The three-loop splitting functions in QCD: the singlet case*, *Nucl. Phys.* **B 691** (2004) 129 [hep-ph/0404111].

[8] R. Hamberg, W.L. van Neerven and T. Matsuura, *A complete calculation of the order α_s^2 correction to the Drell-Yan K factor*, *Nucl. Phys.* **B 359** (1991) 343 *Erratum ibid.* **B 644** (2002) 403.

[9] R.V. Harlander and W.B. Kilgore, *Next-to-next-to-leading order Higgs production at hadron colliders*, *Phys. Rev. Lett.* **88** (2002) 201801 [hep-ph/0201206].

[10] C. Anastasiou, L.J. Dixon, K. Melnikov and F. Petriello, *Dilepton rapidity distribution in the Drell-Yan process at NNLO in QCD*, *Phys. Rev. Lett.* **91** (2003) 182002 [hep-ph/0306192].

[11] C. Anastasiou, L.J. Dixon, K. Melnikov and F. Petriello, *High-precision QCD at hadron colliders: electroweak gauge boson rapidity distributions at NNLO*, *Phys. Rev.* **D 69** (2004) 094008 [hep-ph/0312266].

[12] K. Melnikov and F. Petriello, *The W boson production cross section at the LHC through $O(\alpha_s^2)$*, *Phys. Rev. Lett.* **96** (2006) 231803 [hep-ph/0603182].

[13] C. Anastasiou and K. Melnikov, *Higgs boson production at hadron colliders in NNLO QCD*, *Nucl. Phys.* **B 646** (2002) 220 [hep-ph/0207004].

[14] V. Ravindran, J. Smith and W.L. van Neerven, *NNLO corrections to the total cross section for Higgs boson production in hadron hadron collisions*, *Nucl. Phys.* **B 665** (2003) 325 [hep-ph/0302135].

[15] C. Anastasiou, K. Melnikov and F. Petriello, *Higgs boson production at hadron colliders: differential cross sections through next-to-next-to-leading order*, *Phys. Rev. Lett.* **93** (2004) 262002 [hep-ph/0409088].

[16] C. Anastasiou, K. Melnikov and F. Petriello, *Fully differential Higgs boson production and the di-photon signal through next-to-next-to-leading order*, *Nucl. Phys.* **B 724** (2005) 197 [hep-ph/0501130].

[17] C. Anastasiou, K. Melnikov and F. Petriello, *Real radiation at NNLO: $e^+e^- \to 2$ jets through $O(\alpha_s^2)$)*, *Phys. Rev. Lett.* **93** (2004) 032002 [hep-ph/0402280].

[18] A. Gehrmann-De Ridder, T. Gehrmann and E.W.N. Glover, *Infrared structure of $e^+e^- \to 2$ jets at NNLO*, *Nucl. Phys.* **B 691** (2004) 195 [hep-ph/0403057].

[19] D.A. Kosower, *Antenna factorization of gauge-theory amplitudes*, *Phys. Rev.* **D 57** (1998) 5410 [hep-ph/9710213].

[20] J.M. Campbell, M.A. Cullen and E.W.N. Glover, *Four jet event shapes in electron positron annihilation*, *Eur. Phys. J.* **C 9** (1999) 245 [hep-ph/9809429].

[21] S. Weinzierl, *Subtraction terms at NNLO*, *JHEP* **03** (2003) 062 [hep-ph/0302180].

[22] S. Weinzierl, *Subtraction terms for one-loop amplitudes with one unresolved parton*, *JHEP* **07** (2003) 052 [hep-ph/0306248].

[23] A. Gehrmann-De Ridder, T. Gehrmann and G. Heinrich, *Four-particle phase space integrals in massless QCD*, *Nucl. Phys.* **B 682** (2004) 265 [hep-ph/0311276].

[24] A. Gehrmann-De Ridder, T. Gehrmann and E.W.N. Glover, *Infrared structure of $e^+e^- \to 3$ jets at NNLO: the C_F^2 contribution*, *Nucl. Phys.* **135** *(Proc. Suppl.)* (2004) 97 [hep-ph/0407023].

[25] S. Frixione and M. Grazzini, *Subtraction at NNLO*, *JHEP* **06** (2005) 010 [hep-ph/0411399].

[26] A. Gehrmann-De Ridder, T. Gehrmann and E.W.N. Glover, *Quark-gluon antenna functions from neutralino decay*, *Phys. Lett.* **B 612** (2005) 36 [hep-ph/0501291].

[27] A. Gehrmann-De Ridder, T. Gehrmann and E.W.N. Glover, *Gluon gluon antenna functions from Higgs boson decay*, *Phys. Lett.* **B 612** (2005) 49 [hep-ph/0502110].

[28] A. Gehrmann-De Ridder, T. Gehrmann and E.W.N. Glover, *Antenna subtraction at NNLO*, *JHEP* **09** (2005) 056 [hep-ph/0505111].

[29] S. Weinzierl, *NNLO corrections to 2-jet observables in electron positron annihilation*, *Phys. Rev.* **D 74** (2006) 014020 [hep-ph/0606008].

[30] G. Altarelli and G. Parisi, *Asymptotic freedom in parton language*, *Nucl. Phys.* **B 126** (1977) 298.

[31] F.A. Berends and W.T. Giele, *Multiple soft gluon radiation in parton processes*, *Nucl. Phys.* **B 313** (1989) 595.

JHEP01(2007)070

[32] M.L. Mangano and S.J. Parke, *Multiparton amplitudes in gauge theories*, *Phys. Rept.* **200** (1991) 301 [hep-th/0509223].

[33] A. Gehrmann-De Ridder and E.W.N. Glover, *A complete $O(\alpha\alpha_s)$ calculation of the photon + 1jet rate in e^+e^- annihilation*, *Nucl. Phys.* **B 517** (1998) 269 [hep-ph/9707224].

[34] J.M. Campbell and E.W.N. Glover, *Double unresolved approximations to multiparton scattering amplitudes*, *Nucl. Phys.* **B 527** (1998) 264 [hep-ph/9710255].

[35] S. Catani and M. Grazzini, *Collinear factorization and splitting functions for next-to-next-to-leading order QCD calculations*, *Phys. Lett.* **B 446** (1999) 143 [hep-ph/9810389].

[36] D.A. Kosower, *All-order collinear behavior in gauge theories*, *Nucl. Phys.* **B 552** (1999) 319 [hep-ph/9901201].

[37] S. Catani and M. Grazzini, *Infrared factorization of tree level QCD amplitudes at the next-to-next-to-leading order and beyond*, *Nucl. Phys.* **B 570** (2000) 287 [hep-ph/9908523].

[38] V. Del Duca, A. Frizzo and F. Maltoni, *Factorization of tree QCD amplitudes in the high-energy limit and in the collinear limit*, *Nucl. Phys.* **B 568** (2000) 211 [hep-ph/9909464].

[39] D.A. Kosower, *Multiple singular emission in gauge theories*, *Phys. Rev.* **D 67** (2003) 116003 [hep-ph/0212097].

[40] D.A. Kosower, *All-orders singular emission in gauge theories*, *Phys. Rev. Lett.* **91** (2003) 061602 [hep-ph/0301069].

[41] D.A. Kosower, *Antenna factorization in strongly-ordered limits*, *Phys. Rev.* **D 71** (2005) 045016 [hep-ph/0311272].

[42] Z. Bern, L.J. Dixon, D.C. Dunbar and D.A. Kosower, *One loop n point gauge theory amplitudes, unitarity and collinear limits*, *Nucl. Phys.* **B 425** (1994) 217 [hep-ph/9403226].

[43] Z. Bern, V. Del Duca and C.R. Schmidt, *The infrared behavior of one-loop gluon amplitudes at next-to-next-to-leading order*, *Phys. Lett.* **B 445** (1998) 168 [hep-ph/9810409].

[44] D.A. Kosower and P. Uwer, *One-loop splitting amplitudes in gauge theory*, *Nucl. Phys.* **B 563** (1999) 477 [hep-ph/9903515].

[45] Z. Bern, V. Del Duca, W.B. Kilgore and C.R. Schmidt, *The infrared behavior of one-loop QCD amplitudes at next-to-next-to-leading order*, *Phys. Rev.* **D 60** (1999) 116001 [hep-ph/9903516].

[46] S. Catani and M. Grazzini, *The soft-gluon current at one-loop order*, *Nucl. Phys.* **B 591** (2000) 435 [hep-ph/0007142].

[47] G. Somogyi, Z. Trócsányi and V. Del Duca, *Matching of singly- and doubly-unresolved limits of tree- level QCD squared matrix elements*, *JHEP* **06** (2005) 024 [hep-ph/0502226].

[48] G. Somogyi and Z. Trócsányi, *A new subtraction scheme for computing QCD jet cross sections at next-to-leading order accuracy*, *Acta Phys. Chim. Debr.* **XL** (2006) 101 [hep-ph/0609041].

[49] S. Catani, *The singular behaviour of QCD amplitudes at two-loop order*, *Phys. Lett.* **B 427** (1998) 161 [hep-ph/9802439].

[50] G. Sterman and M.E. Tejeda-Yeomans, *Multi-loop amplitudes and resummation*, *Phys. Lett.* **B 552** (2003) 48 [hep-ph/0210130].

JHEP01(2007)070

[51] F.V. Tkachov, *A theorem on analytical calculability of four loop renormalization group functions*, *Phys. Lett.* **B 100** (1981) 65.

[52] K.G. Chetyrkin and F.V. Tkachov, *Integration by parts: the algorithm to calculate beta functions in 4 loops*, *Nucl. Phys.* **B 192** (1981) 159.

[53] C. Anastasiou, K. Melnikov and F. Petriello, *A new method for real radiation at NNLO*, *Phys. Rev.* **D 69** (2004) 076010 [hep-ph/0311311].

[54] M. Roth and A. Denner, *High-energy approximation of one-loop Feynman integrals*, *Nucl. Phys.* **B 479** (1996) 495 [hep-ph/9605420].

[55] T. Binoth and G. Heinrich, *An automatized algorithm to compute infrared divergent multi-loop integrals*, *Nucl. Phys.* **B 585** (2000) 741 [hep-ph/0004013].

[56] G. Heinrich, *A numerical method for NNLO calculations*, *Nucl. Phys.* **116** *(Proc. Suppl.)* (2003) 368 [hep-ph/0211144].

[57] T. Binoth and G. Heinrich, *Numerical evaluation of phase space integrals by sector decomposition*, *Nucl. Phys.* **B 693** (2004) 134 [hep-ph/0402265].

[58] G. Heinrich, *A numerical approach to infrared divergent multi-parton phase space integrals*, *Nucl. Phys.* **135** *(Proc. Suppl.)* (2004) 290 [hep-ph/0406332].

[59] G. Heinrich, *Towards $e^+e^- \to 3$ jets at NNLO by sector decomposition*, *Eur. Phys. J.* **C 48** (2006) 25 [hep-ph/0601062].

[60] Z. Nagy, *Next-to-leading order calculation of three-jet observables in hadron hadron collision*, *Phys. Rev.* **D 68** (2003) 094002 [hep-ph/0307268].

[61] Z. Nagy and Z. Trócsányi, *Multi-jet cross sections in deep inelastic scattering at next-to-leading order*, *Phys. Rev. Lett.* **87** (2001) 082001 [hep-ph/0104315].

[62] Z. Nagy and Z. Trócsányi, *Next-to-leading order calculation of four-jet observables in electron positron annihilation*, *Phys. Rev.* **D 59** (1999) 014020 [hep-ph/9806317].

JHEP01(2007)070